

Aus der Abt. Vaskuläre Biologie und Tumorangiogenese  
der Medizinischen Fakultät Mannheim  
European Center for Angioscience  
(Direktor: Prof. Dr. Hellmut Augustin)

## Regulation of gluconeogenesis by Aldo-Keto-Reductase 1a1b in zebrafish

Inauguraldissertation  
zur Erlangung des Doctor scientiarum humanarum (Dr. sc. hum.)  
der  
Medizinischen Fakultät Mannheim  
der Ruprecht-Karls-Universität  
zu  
Heidelberg

vorgelegt von  
(Li, Xiaogang)

aus  
(Daqing, China)  
2020

Dekan: Prof. Dr. med. Sergij Goerdts

Referent: Prof. Dr. Jens Kroll

# CONTENT

	Page
LIST OF ABBREVIATIONS .....	1
1 INTRODUCTION .....	4
1.1 Importance of glucose homeostasis .....	4
1.1.1 Hyperglycemia .....	4
1.1.2 Hypoglycemia .....	6
1.2 Regulation of glucose homeostasis .....	7
1.2.1 Glycolysis .....	8
1.2.2 Glycogenesis and glycogenolysis .....	9
1.2.3 Gluconeogenesis .....	9
1.3 Aldo-keto reductase (Akr) superfamily .....	10
1.3.1 Function of Akr1a1 .....	12
1.3.2 Novel functions of Akr1a1 .....	13
1.3.3 <i>Akr1a1</i> in zebrafish .....	14
1.4 Aim of this study .....	15
2 MATERIAL AND METHODS .....	16
2.1 Material .....	16
2.1.1 Equipment .....	16
2.1.2 Chemicals .....	17
2.1.3 Consumables .....	17
2.1.4 Buffers and Solutions .....	18
2.1.5 Kits and Reagents .....	21
2.1.6 Oligonucleotides .....	21
2.1.7 Antibodies .....	22
2.1.8 Zebrafish transgenic lines .....	23
2.2 Methods .....	23

2.2.1	Animal studies.....	23
2.2.1.1	Ethics.....	23
2.2.1.2	Zebrafish maintenance .....	23
2.2.1.3	Incubation of zebrafish embryos/larvae .....	23
2.2.1.4	Microscopy and analysis of pronephric alternations in larvae.....	23
2.2.1.5	Determination of pronephros function.....	24
2.2.1.6	Dissection of adult zebrafish.....	24
2.2.1.7	Histology (Periodic acid-Schiff).....	24
2.2.1.8	Measurement of adult zebrafish blood glucose .....	25
2.2.2	Molecular biology .....	26
2.2.2.1	Isolation of genomic DNA .....	26
2.2.2.2	Polymerase chain reaction (PCR) .....	26
2.2.2.3	DNA gel electrophoresis .....	27
2.2.2.4	RNA isolation from larvae and adult zebrafish organs.....	27
2.2.2.5	cDNA synthesis from RNA (RT-PCR).....	27
2.2.2.6	Real-time quantitative PCR (RT-qPCR) .....	27
2.2.2.7	Western blot analysis .....	28
2.2.2.8	Immunohistochemistry.....	28
2.2.3	Biochemical analysis.....	29
2.2.3.1	Determination of activity of Ak, ALDH and Glo1 enzymes.....	29
2.2.3.2	Determination of methylglyoxal (MG), 3-Deoxyglucosone (3-DG), and glyoxal	29
2.2.3.3	Metabolomic analysis .....	30
2.2.3.4	Measurement of glutamate and alanine in adult zebrafish kidneys and livers	31
2.2.4	Statistical analysis.....	31
3	RESULT .....	32
3.1	Expression of Ak1a1b in zebrafish .....	32
3.2	Generation and validation of <i>akr1a1b</i> <sup>-/-</sup> mutants.....	34
3.3	<i>Akr1a1b</i> knock-out in zebrafish caused alterations of the embryonic pronephros and of adult kidneys .....	36
3.4	Glutamate accumulated in <i>akr1a1b</i> <sup>-/-</sup> zebrafish and caused pronephros alterations.....	41

3.5	Altered gluconeogenesis in <i>akr1a1b</i> <sup>-/-</sup> zebrafish .....	46
3.6	Akr1a1b regulates S-nitrosylation.....	48
4	DISCUSSION .....	51
4.1	<i>Akr1a1b</i> expression in zebrafish.....	52
4.2	<i>Akr1a1b</i> deficiency affects zebrafish renal development and functionality by accumulating glutamate .....	53
4.3	Inhibitory of gluconeogenesis leads to the glutamate accumulation .....	55
4.4	Akr1a1b regulates S-nitrosylation.....	56
5	SUMMARY .....	59
6	REFERENCE .....	60
7	CURRICULUM VITAE .....	74
8	ACKNOWLEDGEMENTS.....	75

## LIST OF ABBREVIATIONS

°C	Degree celsius
∞	Forever
μl	Microliter
μm	Micrometre
μM	Micromolar
%	Percent
3-DG	3-deoxyglucosone
ADP	Adenosine diphosphate
AGE	Advanced glycation end-product
Akr	Aldo-keto reductase
ALDH	Aldehyde dehydrogenase
AMP	Adenosine monophosphate
ANOVA	Analysis of variance
ATP	Adenosine triphosphate
cDNA	Complementary DNA
CoA	Coenzyme A
CRISPR	Clustered regularly interspaced short palindromic repeats
DAG	Diacylglycerol
DB	1,2-diaminobenzene
DETAPAC	Diethylenetriaminepentaacetic acid
DHAP	Dihydroxyacetone phosphate
DNA	Deoxyribonucleic acid
ECL	Chemiluminescence
EDTA	Ethylenediaminetetraacetic acid
EGFP	Enhanced green fluorescent protein
EM	Electron microscope
F1,6BP	Fructose 1,6-bisphosphate
F6P	Fructose 6-phosphate
FAME	Fatty acid methyl ester
FBS	Fetal bovine serum

## Abbreviations

---

GAPDH	Glyceraldehyde 3-phosphate dehydrogenase
GC/MS	Gas chromatography-mass spectrometry
GDM	Gestational diabetes
GFP	Green fluorescent protein
GHB	Hydroxybutyrate
Gln	Glutamine
Glo1	Glyoxalase I
Glu	Glutamic acid
GLUT	Glucose transporters
HK	Hexokinase
hpf	Hours post fertilization
hpi	Hours post injection
HPLC	High-performance liquid chromatography
HRP	Horseradish peroxidase
LC-MS/MS	Liquid chromatography–mass spectrometry
L-NAME	N omega-Nitro-L-arginine methyl ester hydrochloride
MEFs	Mouse embryonic fibroblasts
MG	Methylglyoxal
MSG	Monosodium glutamate
MSTFA	N-methyl-N-(trimethylsilyl)trifluoroacetamide
NAD <sup>+</sup>	Nicotinamide adenine dinucleotide
NADH	Nicotinamide adenine dinucleotide hydrate
NADP	Nicotinamide adenine dinucleotide phosphate
NADPH	Nicotinamide adenine dinucleotide phosphate hydrate
NP40	Nonidet P-40
P	Phosphate
PAS	Periodic acid-Schiff
PBS	Phosphate-buffered saline
PCR	Polymerase chain reaction
PEPCK	Phosphoenolpyruvate-carboxykinase
PFA	Paraformaldehyde
PFK	Phosphofructokinase
PK	Pyruvate kinase

## Abbreviations

---

PKC	Protein kinase C
PKM2	Pyruvate kinase M2
PTU	1-phenyl-2-thiourea
qPCR	Quantitative polymerase chain reaction
RNA	Ribonucleic acid
ROS	Reactive oxygen species
RT-PCR	Reverse transcription polymerase chain reaction
SCoR	S-nitroso-coa reductase
SDS-PAGE	Sodium dodecyl sulfate–polyacrylamide gel electrophoresis
S-NO	S-nitrosylated
SNOs	S-nitrosylated proteins
SSA	Succinic semialdehyde
T1DM	Type 1 diabetes
T2DM	Type 2 diabetes
TAE	Tris-acetate-EDTA
TBME	Tert-butyl methyl ether
UDP	Uridine diphosphate
UDP-GlcNAc	Udp-nacetylglucosamine
UPLC-FLR	Ultra-performance liquid chromatography with fluorescence
WHO	World health organization



# 1 INTRODUCTION

## 1.1 Importance of glucose homeostasis

Carbohydrates are the most abundant biomolecules on earth. Among numerous carbohydrates, the simplest form and the most basic unit is the monosaccharide, also called simple sugar, including glucose, fructose, galactose, etc. Although some fungi use sucrose<sup>(Lin et al., 2010)</sup> or maltose<sup>(Xiao et al., 2004)</sup> as primary carbohydrate sources, glucose is generally considered as the most important energy resource material for most livings, from bacteria to humans. In humans, glucose is mainly transported through the cardiovascular circulation system in the blood, subsequently called blood glucose. This glucose comes from food we eat, and our body can also release produced glucose into the circulation which comes from livers and kidneys. Blood glucose mainly takes the responsibility of energy metabolism and maintains normal cellular functions in all organs, commonly used as a clinical parameter to diagnose metabolic diseases.

### 1.1.1 Hyperglycemia

Although glucose is essential for living, continuously increased or decreased blood glucose levels could lead to several metabolic diseases. For example, diabetes, a severe and chronic disease characterized by high blood glucose, also called hyperglycemia<sup>(Cho et al., 2018)</sup>, which caused 4.2 million deaths in 2019. As recommended by WHO, more than 7.0 mmol/L (126 mg/dl) of fasting blood glucose or more than 11.1 mmol/L (200 mg/dl) of 2 hours postprandial blood glucose could be diagnosed as diabetes<sup>(Roglic and World Health Organization, 2016)</sup>.

Currently, as recommend by WHO, two main types of diabetes are clarified: (1) Type 1 diabetes (T1DM) is thought to be caused by an autoimmune reaction, it starts mostly in childhood and early adulthood, but can develop at any age. Hyperglycemia caused by T1DM results from the failure of the pancreatic  $\beta$  cells, thereby leads to absolute insulin deficiency<sup>(Katsarou et al., 2017)</sup>. (2) Type 2 diabetes (T2DM) is the most common type of diabetes, accounts for 90%-95% of all diabetic patients. T2DM is most common in adults, but recently increasing numbers of children and adolescents suffering from T2DM have been reported<sup>(Roglic and World Health Organization, 2016)</sup>. Hyperglycemia caused by T2DM results

## Introduction

---

from insulin resistance with relative insulin deficiency<sup>(Petersmann et al., 2019)</sup>. However, because of the higher prevalence of obesity in recent years, the distinction between these two types of diabetes becomes less obvious. Moreover, there are many other subtypes of diabetes, like slowly evolving immune-mediated diabetes<sup>(Atkinson et al., 2014)</sup>, ketosis-prone T2DM<sup>(Sobngwi et al., 2002)</sup>, monogenic diabetes<sup>(Hattersley et al., 2009)</sup>, and gestational diabetes (GDM)<sup>(Bellamy et al., 2009)</sup>.

Several prospective clinical studies showed strong relationships between hyperglycemia and micro- or macrovascular complications<sup>(Borg et al., 2011; Diabetes et al., 1993; Duckworth et al., 2009; UKPDS, 1998)</sup>, including but not limited to kidney failure, vision loss, limb amputation, nerve damage, heart attack, and stroke<sup>(Forbes and Cooper, 2013)</sup>. The hyperglycemic induced metabolic changes have been identified as one crucial damaging mechanism and caused an additional 2.2 million deaths<sup>(Roglic and World Health Organization, 2016)</sup>.

Currently, four main hypotheses were proposed for diabetic complications as mentioned earlier of which are all potentially initiated by hyperglycemia (Fig. 1)<sup>(Brownlee, 2001)</sup>: (1) Increased polyol pathway flux: intracellular aldose reductase would be upregulated under the hyperglycemic environment, resulting in more glucose conversion to sorbitol, and the sorbitol is further oxidized to fructose. The increased polyol pathway flux induced higher reactive oxygen species<sup>(Rittner et al., 1999)</sup>, osmotic stress, and cytosolic NADH:NAD<sup>+</sup> ratio<sup>(Ramasamy and Goldberg, 2010)</sup>. (2) Increased advanced glycation end-product (AGE) formation: intracellular hyperglycemia leads to more intracellular and extracellular AGEs formation. All three main AGE precursors, glyoxal, 3-deoxyglucosone, and methylglyoxal, can modify proteins in intracellular and extracellular cellular compartments or in plasma, For example, bFGF, is one of the main AGE-modified proteins in endothelial cells. AGE-bFGF alters vascular cell functions since bFGF plays an essential role in cell proliferation and basement membrane production<sup>(Giardino et al., 1994)</sup>. (3) Activation of protein kinase C (PKC) isoforms: intracellular hyperglycemia increases the amount of diacylglycerol, thereby activating PKC, both *in vivo* and *in vitro* studies. Abnormal activation of PKC has been implicated in nephropathy<sup>(Craven et al., 1994)</sup> and in vascular alterations<sup>(Hempel et al., 1997; Williams et al., 1997)</sup>. (4) Increased hexosamine pathway flux: only 1%-3% of glucose is metabolized into the hexosamine pathway under normal conditions producing UDP N-acetyl glucosamine (UDP-GlcNAc), but highly increased

## Introduction

under diabetic conditions. The UDP-GlcNAc interacts for example with transcription factor  $\beta$  (TF $\beta$ ) (Wells and Hart, 2003), specificity protein 1 (Sp1) (Chen et al., 1998), resulting in many alterations in glucose-responsive genes expression and protein function, thereby inducing diabetic complications.

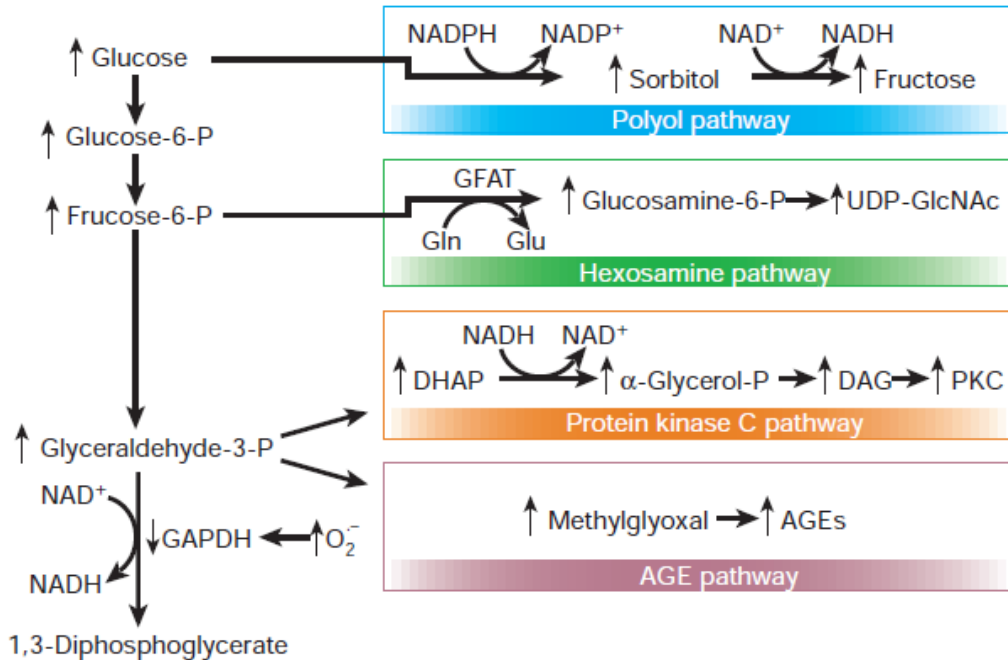


**Figure 1. Potential mechanism by which hyperglycemia-induced four pathways of hyperglycemic damage.**

NADPH: Nicotinamide adenine dinucleotide phosphate hydrate, NADP: Nicotinamide adenine dinucleotide phosphate, NAD<sup>+</sup>: Nicotinamide adenine dinucleotide, NADH: Nicotinamide adenine dinucleotide hydrate, Gln: Glutamine, Glu: Glutamic acid, UDP-GlcNAc: UDP-Nacetylglucosamine, DHAP: Dihydroxyacetone phosphate, DAG: diacylglycerol, PKC: Protein kinase C, AGE: Advanced glycation endproduct, P: Phosphate, GAPDH: glyceraldehyde 3-phosphate dehydrogenase. Figure and legend by Brownlee, M. (2001). *Biology of Diabetic Complications*. Nature 414, 813–820, with permission for reprint by Springer Nature and Copyright Clearance Center)

### 1.1.2 Hypoglycemia

In contrast, hypoglycemia also called low blood glucose, in which the range is defined variable. In adults, plasma glucose concentration of less than 3.9 mmol/L (70 mg/dL) of diabetic patients or less than 3.0 mmol/L (55 mg/dL) of people without diabetes are defined (Cryer et al., 2009). In neonates, the threshold is debatable and elusive. Some studies

## Introduction

---

suggest hypoglycemia as a plasma glucose concentration of less than 1.65 mmol/L (30 mg/dL) in the first 24 hours of life and less than 2.5 mmol/L (45 mg/dL) after that (Cornblath and Ichord, 2000); nevertheless, the level less than 2.6 mmol/L (47 mg/dL) is commonly practical used (Stomnaroska-Damcevski et al., 2015) in the clinic.

Hypoglycemia rarely appears in people who do not have diabetes. Although some severe illnesses may also result in hypoglycemia, like insulinoma, non-islet cell tumors, hormone deficiencies, liver or kidney failure (Kittah and Vella, 2017), the most common cause of hypoglycemia is an inappropriate insulin or medicine usage (Yanai et al., 2015). Physiologically, hypoglycemia is not a disease, but it may indicate a health problem. In the adult body, the nervous system demands glucose at the highest level of all organs (Howarth et al., 2012). The brain is a nerve cell-rich organ which consumes approximately 20% of glucose-derived energy (Mergenthaler et al., 2013) and requires 130 g glucose a day (Cunnane et al., 2011). Therefore, if the amount of glucose fueled by the blood falls, the brain will be one of the first affected organ, accompanying nausea, trembling, and sweating (Tesfaye and Seaquist, 2010). Under diabetic conditions, insufficient glucose supplement to the brain can cause to a series of consequences, for example, impaired awareness (Little et al., 2018), cognitive dysfunction (Cukierman-Yaffe et al., 2019), dementia (Whitmer et al., 2009), seizure (Buckingham et al., 2008), and even brain death (Cryer, 2007). Likewise, other organs also can be harmed by hypoglycemia. Diabetic patients accompanied by severe hypoglycemia can suffer from increased coronary artery calcification (Saremi et al., 2016), longer diabetes duration, higher incidence of heart failure and kidney disease, greater risk of cardiovascular events (Zinman et al., 2018) and even death (Finfer et al., 2012).

These studies strongly suggest that maintaining physiological glucose concentrations within narrow limits is fundamental for life and long-term health. The process of maintaining blood glucose at a steady-state level is called glucose homeostasis.

### 1.2 Regulation of glucose homeostasis

Regulation of glucose homeostasis is a fundamental process to maintain blood glucose at a physiological level. Glucose homeostasis is tightly regulated by several hormonal, neural, and substrate glucoregulatory factors through glucose catabolism (metabolizing) and anabolism (producing) pathways. The central glucose metabolizing pathways are

glycolysis and glycogenesis, while glucose producing pathways are glycogenolysis and gluconeogenesis (Alsahli and Gerich, 2017; Petersen et al., 2017).

### 1.2.1 Glycolysis

Glycolysis is a universal pathway in all living cells of the body. It mostly occurs in the cytosol of cells and converts glucose into pyruvate. Afterward, pyruvate can be catalyzed to lactate or organic acids in the absence of oxygen, or catalyzed to acetyl-CoA in the presence of oxygen, respectively. Then, the acetyl-CoA enters the citric acid cycle and oxidative phosphorylation to generate energy for bioenergetic homeostasis and the survival of all cells occurs.

On the one hand, for the short term, consumption of ATP, reproduction of NADH, and three allosteric enzymes, hexokinase/glucokinase (HK/GK), phosphofructokinase (PFK), and pyruvate kinase (PK), synergistically regulate glycolysis. Hexokinase catalyzes glucose to glucose-6-phosphate (G-6-P) in the first step of glycolysis. However, hexokinase is inhibited allosterically by increased concentrations of glucose-6-phosphate. The PFK1 plays the most critical role in glycolysis, converts fructose-6-phosphate (F-6-P) and ATP to fructose1,6-bisphosphate (F1,6BP) and ADP. PFK1 is allosterically inhibited by high ATP levels but activated by a high AMP concentration; nevertheless, the most potent activator is fructose 2,6-bisphosphate (F2,6BP), which is produced by PFK2. Lastly, PK is allosterically inhibited by high ATP levels too, thereby regulating glycolysis. Moreover, HK and PK can be activated by the PFK enzyme.

On the other hand, glucagon, epinephrine, and insulin affect glycolytic rate for long term regulation. In adipose and muscle, insulin promotes glucose entry into the cells by activating PI3K and MAPK pathways. Although the glucose uptake does not alter in the liver cells, glucose release is suppressed by insulin. Moreover, insulin dephosphorylates PFK2, which elevates F2,6BP in the liver and, therefore, activates glycolysis<sup>(Wu et al., 2005)</sup>. Glycolysis also can be regulated by glucose transporters (GLUT) since the cellular uptake of glucose by GLUT occurs in response to insulin signals<sup>(Rui, 2014; Vargas et al., 2020)</sup>. Conversely, glucagon, as a counter regulatory hormone for insulin, can inhibit glycolysis by inhibiting PFK2, decreasing F2,6BP via PKA pathway<sup>(Jiang and Zhang, 2003)</sup>.

### 1.2.2 Glycogenesis and glycogenolysis

Glycogenesis and glycogenolysis coordinately determine the deposit of glycogen *in vivo* and keep the balance of blood glucose under fasting and postprandial states. Glycogenesis is the process of glycogen synthesis, in which excessive glucose is added to glycogen chains for storage in skeletal muscle and liver cells, thereby decreasing blood glucose postprandial. By contrast, glycogenolysis is the process of glycogen breakdown in skeletal muscle and liver cells during the period of fasting and exercising for increasing blood glucose. Both glycogenolysis and glycogenesis are subject to complex regulatory mechanisms.

On the one hand, glycogenesis is primarily regulated by glycogen synthase activity, which is allosteric activated by glucose 6-phosphate and inactivated by its phosphorylation. On the other hand, the phosphorylation of glycogen phosphorylase regulates the glycogenolytic flux. Both glycogen synthase and glycogen phosphorylase could be dephosphorylated by insulin via the Akt/PKB signaling pathway, (Flannery et al., 2018; Petersen et al., 2017), in contrast, phosphorylated by glucagon via several kinases, including PKA. (Jiang and Zhang, 2003).

### 1.2.3 Gluconeogenesis

Gluconeogenesis, contrary to glycolysis, is a glucose-producing process that mainly uses specific non-carbohydrate carbon substrates, like lactate, glycerol, or glucogenic amino acids (Yip et al., 2016). Gluconeogenesis is one of several main mechanisms used by humans and many other animals to maintain blood glucose levels, particularly under long-term fasting conditions. It has been found that gluconeogenesis accounts for approximately 50% of all circulation glucose-releasing in overnight-fasted humans (Chandramouli et al., 1997), and up to 96% when fasting period lasted to 40 hours (Rothman et al., 1991).

It had long been postulated that the liver is the sole source of glucose generation, but this hypothesis was disapproved by observations that the mammalian renal cortical tissue can perform gluconeogenesis *in vitro*, in animals and humans (Benoy and Elliott, 1937; Bergman and Drury, 1938; Bjorkman et al., 1979; Drury et al., 1950). Increasing evidence supports the hypothesis that the kidney plays a vital role in glucose homeostasis via gluconeogenesis,

especially in the prolonged fasting state<sup>(Gerich et al., 2001)</sup>. Gluconeogenesis shows a reciprocal regulation with glycolysis and is on different levels regulated. One regulation relates to glucagon induced gene expression of key regulating enzymes Phosphoenolpyruvate-carboxykinase (PEPCK) and Glucose 6-phosphatase, while allosteric regulation of Fructose-1,6-bisphosphatase is mediated by fructose-2,6-bisphosphate, AMP, and ADP<sup>(Li et al., 2020)</sup>. Insulin inhibits liver and renal gluconeogenesis by suppressing the expression of PEPCK and glucose-6-phosphatase via the PI3K-AKT pathway<sup>(Barthel and Schmoll, 2003; Pina et al., 2020)</sup>. In contrast, glucagon activates cAMP/PKA, thereby increasing the expression of PEPCK and glucose-6-phosphatase in the liver. However, after the glucagon treatment, either renal gluconeogenesis or renal glucose release was not induced<sup>(Stumvoll et al., 1998)</sup>. Interestingly, later studies have identified a substrate preference for gluconeogenesis in different organs; explicitly, the liver prefers alanine while the kidney prefers glutamate <sup>(Stumvoll et al., 1999)</sup>.

### 1.3 Aldo-keto reductase (Akr) superfamily

Aldo-keto reductase is a superfamily containing over 180 family members, which is subdivided into 16 categories by sequence alignment, protein function, and structural comparison<sup>(Penning, 2015)</sup>. Although all these over 180 members are not catalyzing the same substrates like some enzymes transform glucose<sup>(Bohren et al., 1989)</sup>, some catalyze lipid aldehydes<sup>(Srivastava et al., 1995)</sup>, or ketosteroids<sup>(Penning et al., 2000)</sup>, carcinogen metabolites<sup>(Palackal et al., 2002)</sup>, all Aldo-keto reductase enzymes possess a similar structure characterization. They were identified as a kind of NAD(P)(H) dependent nucleotide-binding protein characteristically  $\beta - \alpha - \beta$  fold, which comprises a parallel  $(\alpha/\beta)_8$ -barrel with a novel NADP-binding motif<sup>(Schade et al., 1990)</sup>. Besides, substrates are bound in an extended conformation. The binding site always locates in the elliptical pocket at the back of the barrel in the C-terminal end of the  $\beta$  sheet.

However, only 15 Akrs exist in humans<sup>(Hyndman et al., 2003)</sup>. The functions of the Akr gene families have mostly been mysterious. Akr1b1 enzyme is the one who has attracted the most attention of all Akr gene families in the past because it was recognized as a rate-limited enzyme of the polyol pathway, where glucose could be transformed into sorbitol, which later oxidizes to fructose <sup>(Hers, 1956)</sup>. Further, fructose cause a serious of secondary diabetic complications, including but not limited to retinopathy<sup>(Lorenzi, 2007; Obrosova et al., 2010)</sup>,

## Introduction

---

nephropathy<sup>(Dunlop, 2000)</sup>, neuropathy<sup>(Oates, 2008)</sup>, and cardiovascular disease<sup>(Li et al., 2008)</sup>. Several theories may explain the mechanisms. The disruption of osmotic equilibrium caused by more polyol flux was viewed as the main reason for diabetic cataract<sup>(Kinoshita and Nishimura, 1988)</sup>. The polyol pathway also contributed to the inducing of oxidative stress by altering the NADPH/NADP ratio and glutathione/oxidized glutathione (GSH/GSSG) ratio, which lead to diabetic cataract and neuropathy<sup>(Chung et al., 2003; Srivastava et al., 2005)</sup>. The fructose and its metabolites fructose-3-phosphate and 3-deoxyglucosone (3DG), are more effective than glucose to glycating proteins to the formation of AGEs<sup>(Hamada et al., 1996; Szwergold et al., 1990)</sup>. Moreover, The polyol pathway can activate PKC that damage vasculature and nerves<sup>(Amara et al., 2019; Paul et al., 2020)</sup>.

Many *in vivo* studies in animals showed that knock-out or inhibition of Akr1b1 prevents the development of diabetic complications, like cataractogenesis<sup>(Cogan et al., 1984; Lou et al., 1996)</sup>, retinopathy<sup>(Kato et al., 2003; Toyoda et al., 2014)</sup>, nephropathy<sup>(Beyer-Mears et al., 1988; He et al., 2019; Tilton et al., 1989)</sup>, and neuropathy<sup>(Asano et al., 2019; Bril et al., 2009; Li et al., 2016)</sup>. It appeared that Akr1b1 inhibitors would be potent drugs for treating diabetes in humans; however, they failed in clinical trials because of their high incidence of adverse effects and ineffectiveness<sup>(Suzen and Buyukbingol, 2003)</sup>. One of the likely reasons for the failure of human treatment is that many Akr1b1 inhibitors, like sorbinil, alrestatin, and quercitrin, will also inhibit Akr1a1 in several tissues<sup>(El-Kabbani and Podjarny, 2007; Srivastava et al., 1982)</sup>. Therefore we assumed that Akr1a1 plays important physiological roles, so that the inhibitory of Akr1a1 caused severe side effects by Akr1b1 inhibitors treatment.

Akr1b10, which is primarily expressed in the adrenal gland, small intestine, and colon<sup>(Fagerberg et al., 2014)</sup>, has developed as a potential biomarker for the diagnosis and prognosis of several cancers, like hepatocellular carcinoma<sup>(DiStefano and Davis, 2019; Liu et al., 2012)</sup>, smoking-related lung adenocarcinomas<sup>(Fukumoto et al., 2005)</sup>, cholangiocarcinomas<sup>(Heringlake et al., 2010)</sup>, breast carcinomas<sup>(Ma et al., 2012)</sup>. It has been reported that the overexpression of Akr1b10 in tumor cells is one reason for their drug-resistant because Akr1b10 can catalyze antitumor antibiotics, e.g., daunorubicin, to the inactive form so that tumor cell survive under treatment<sup>(Balendiran, 2009)</sup>. Therefore, Akr1b10 inhibitor appears likely that as novel antitumor drugs<sup>(Huang et al., 2016)</sup>.



### 1.3.1 Function of Akr1a1

Akr1a1's molecular weight is 36kDa and consists of 325 amino acids, which folds into an 8-stranded parallel  $\beta$  /  $\alpha$  barrel<sup>(El-Kabbani et al., 1994)</sup>. Akr1a1 enzyme exists in virtually every tissue in humans with the highest level in the kidney<sup>(Fagerberg et al., 2014)</sup>. It has a suggested major function in reducing biogenic and xenobiotic aldehyde (with preference to aromatic aldehydes<sup>(Markus et al., 1983)</sup>), to their corresponding alcohols in an NADPH-dependent manner, which is different with Akr1b1, which uses both NADPH and NADH as cofactors. Additionally, Akr1a1 is well known as a critical enzyme of ascorbic acid biosynthesis in mouse by converting D-glucuronate to L-gluconate<sup>(Gabbay et al., 2010)</sup>. Akr1a1 deficiency results in severe osteopenia and spontaneous fractures in mice due to the absence of ascorbic acid<sup>(Lai et al., 2017; Takahashi et al., 2012)</sup>. Although this pathway does not exist in humans, more studies showed that Akr1a1 could play a role as detoxifying enzymes in humans and other animals. Akr1a1 can catalyze Benzo[a]pyrene-7,8-diol to the reactive and redox-active Benzo[a]pyrene-7,8-dione in human bronchoalveolar H358 cells<sup>(Jiang et al., 2006)</sup> under the redox state of cells<sup>(Jiang et al., 2005)</sup>; exogenous gamma-hydroxybutyrate (GHB) to succinic semialdehyde (SSA) in human HepG2 cells<sup>(Alzeer and Ellis, 2014)</sup>. When Akr1a1 is overexpressed, mouse embryonic fibroblasts (MEFs) showed a stronger ability to reduce methylglyoxal and acrolein and became more resistant to cytotoxic agents, such as acrolein. Also, endoplasmic reticulum stress and protein carbonylation induced by acrolein treatment were attenuated in Akr1a1 overexpressed MEFs<sup>(Kurahashi et al., 2014)</sup>. Conversely, knock-down of *akr1a1* resulted in less resistance of H<sub>2</sub>O<sub>2</sub> and 4-hydroxynonenal-induced cytotoxicity meanwhile increased ROS level in 1321N1 cells<sup>(Li et al., 2013)</sup>.

Interestingly and unexpectedly, the knock-down of *akr1a1* in human HepG2 cells also led to a significant reduction of GHB-dehydrogenase activity when treated with high concentration (10mM) of GHB, and of SSA reductase activity treated with high level (1mM) of SSA<sup>(Alzeer and Ellis, 2014)</sup>. These phenomena suggested that the Akr1a1 enzyme may be involved in mechanisms regulating other proteins' activities.

## 1.3.2 Novel functions of Akr1a1

However, no evidence could prove that the Akr1a1 enzyme regulates the activity of other enzymes until a recent study identified mouse Akr1a1 acting as S-nitroso-glutathione reductase<sup>(Stomberski et al., 2019)</sup> and S-nitroso-CoA reductase (SCoR)<sup>(Zhou et al., 2019)</sup>. Together, these studies suggested that the Akr1a1 enzyme could extensively regulate protein s-nitrosylation. Akr1a1 removes SNO from proteins, thereby inhibiting the S-nitrosylation process (Fig. 2). The most important finding of these studies is that it was shown that the activity of the rate-limited enzyme in glycolysis, pyruvate kinase M2 (PKM2), can be regulated by S-nitrosylation programming. In detail, *akr1a1* knocked-out mice displayed enhanced S-nitrosylation of renal PKM2 that inhibited its activity by blocking tetramer formation, subsequently hindering the glycolysis process, which was presented by increased multiple glycolytic intermediates but with no alteration of pyruvate. The accumulated intermediates entered into the pentose phosphate pathway (PPP), thereby generating NADPH, increasing glutathione (GSH), activating antioxidant enzymes, and protecting the kidney from acute kidney injury in further.<sup>(Zhou et al., 2019)</sup>.

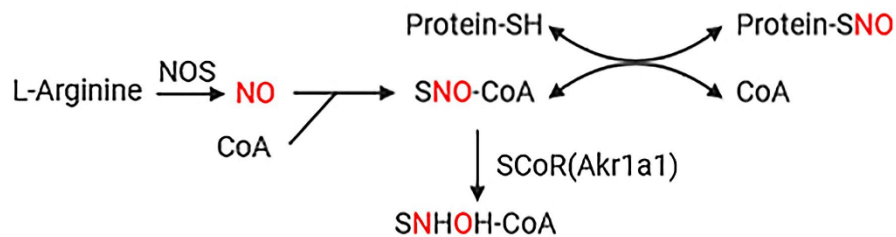


**Figure. 2 SNO-CoA-SCoR (Akr1a1) system.**  
mechanism of how Akr1a1 regulates protein S-nitrosylation

1.3.3 *Akr1a1* in zebrafish

As widely existed enzymes, Akr families also exist in zebrafish. Based on the database analysis, we can only find the following *akr* genes in zebrafish: *akr1a1*, *akr1b1*, and *akr7a3* (Fig. 3). However, unlike other animals, two separate *akr1a1* genes exist simultaneously in zebrafish, namely *akr1a1a* and *akr1a1b*, and whose functions have not been studied yet.

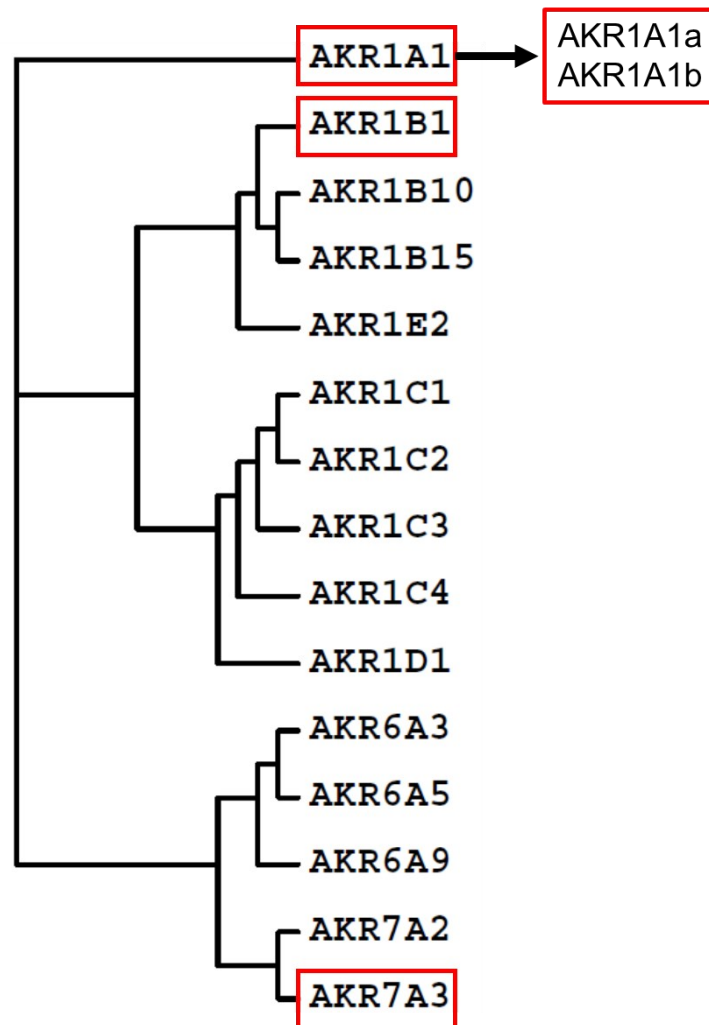


**Figure. 3 Zebrafish display orthologues of human Akr proteins.**

Phylogenetic tree of 15 well-known and characterized human proteins of three Akr categories. Additionally, zebrafish show two paralogues for Akr1a1. Red boxes mark the Akr orthologues in zebrafish.

### 1.4 Aim of this study

The zebrafish has been established as a model for diabetes research in the past decades<sup>(Heckler and Kroll, 2017; Lodd et al., 2019; Schmohl et al., 2019; Wiggenhauser et al., 2020)</sup>, because glucose homeostasis in zebrafish is very similar to humans and other mammals. Alterations in glucose homeostasis are commonly associated with organ damage, including the kidney, eyes, vasculature, and nerves<sup>(Olsen et al., 2010)</sup>. Previous research has revealed that inhibition of the Akr1a1 enzyme alters glycolysis by regulating S-nitrosylation of PKM2, therefore regulating glucose homeostasis. However, few studies focused on the function of Akr1a1b enzyme in zebrafish.

Thus, this study aims to evaluate whether Akr1a1b regulates glucose homeostasis in zebrafish and investigate its mechanisms. The zebrafish *akr1a1b* knockout was generated by my colleague Dr. Felix Schmoebl. My objective was:

1. Determine the alteration of kidney morphology in embryonic, larval, and adult mutant zebrafish via fluorescent microscopy and histology technology;
2. Determine the metabolome and transcriptome alterations in larval and adult mutant zebrafish by targeted/ semi-targeted analyses of metabolites and qPCR technology;
3. Investigate the mechanisms of all alterations and thereby identity the function of Akr1a1b in zebrafish.

## 2 MATERIAL AND METHODS

### 2.1 Material

#### 2.1.1 Equipment

Products	company
Analytical balance ABS-N_ABJ-NM_ACS_ACJ	Kern & Sohn
BioPhotometer® D30	Eppendorf
Dry bath incubator	Major Science
FreeStyle Freedom Lite - blood glucose monitoring system	Abbott
Hamilton 1705 Gastight Syringe, 50 uL	Hamilton
Jun-Air 3-4 Quiet Running Compressor	Jun-Air
Leica HI1210 Water bath for paraffin sections	Leica
Leica RM2235 Manual Rotary Microtome	Leica
Mikro 200/200r Microlitre Centrifuges	Andreas Hettich
Mini centrifuge ROTILABO®	Carl Roth
P-30 vertical micropipette puller	Sutter instruments
Perfect Blue™ Gel System	Peqlab Biotechnologie
Power Supplies EV231	Consort
ProfiLine pH/mV-Meter pH 197i	WTW
PV820 Pneumatic Picopump	World Precision Instruments (WPI)
QuantStudio 3 Real-Time-PCR-System	Applied Biosystems
Rotina 420 & 420R Benchtop Centrifuge	Andreas Hettich
See-saw rocker SSL4	Stuart
T100 PCR thermal cycler	BioRad
Universal Oven Model UN30	Memmert
Universal Oven Model UNB 300	Memmert
UV transilluminator	INTAS
Water Bath WB12	M-L Tech Mess- & Labortechnik
Axio Scan. Z1	Carl Zeiss Microscopy

## Material and methods

---

### 2.1.2 Chemicals

If not indicated otherwise, all chemicals used during the experiments were purchased from the

following companies:

Carl Roth GmbH & Co. KG

Merck AG

Roche Diagnostics GmbH

Sigma-Aldrich Chemie GmbH

Thermo Fisher Scientific Inc.

### 2.1.3 Consumables

<b>Products</b>	<b>Company</b>
0.2 mL 8-Strip PCR Tubes	Star Labs
6/96-Well Culture Plate	Greiner Bio-one
Blood glucose test stripes	Abbott (FreeStyle Lite)
Borosilicate Glass Cylinders (14 mm I.D. x 5 mm)	Biotechs
Cover Glasses, 22 x 22 mm	Menzel Gläser
Dumont Forceps, No. 5	NeoLabs
Falcon® 15/50 mL Polystyrene Centrifuge Tube	Corning
Feather Sterile Disposable Scalpels, No.10/11	Feather
Filter tips PP (1000, 100, 20 and 10 µl)	Nerbe plus GmbH
Food spoons (2.5 mL, blue, sterile)	bürkle
Graduated TipOne Tip, refill (1000, 200, 10 µL)	Star Labs
High Precision Microscope Cover Glasses	Deckgläser
Micro scissors high precision, 105 mm, 15 mm	Carl Roth
MicroAmp® Fast Optical 96-Well Reaction Plate	Applied Biosystems
Needle 20G x1 ½" nr.1	BD Microlance
Nitrile Gloves	Semperguard
PAP pen	abcam
Petri dish, 100/20 mm	Greiner Bio-one

## Material and methods

---

Pipettes (P1000, P200, P20, P10 and P2)	Gilson/Eppendorf
Safe-Lock tubes (0.5, 1.5 and 2.0 mL)	Eppendorf
Standard Pastette NS	alpha laboratories
Superfrost Plus™ Adhesion Microscope Slides	Thermo Fisher
Syringe filters ROTILABO® MCE, 0.45 µm	Carl Roth
Syringes (1 mL, 30 mL)	BD Plastipak
Thin-Wall capillary TW100F-4	World Precision Instruments (WPI)

### 2.1.4 Buffers and Solutions

Name	Recipe
10x PBS	80g NaCl 2g KCl 11.5g Na <sub>2</sub> HPO <sub>4</sub> 2g KH <sub>2</sub> PO <sub>4</sub> Add distilled water to a final volume of 1 L
50x TAE buffer	232 g Tris 57.1 mL conc. acetic acid 100 mL 0.5 M EDTA, pH 8.6 Add distilled water to a final volume of 1 L
NP40 lysis buffer	0.87g NaCl 5ml 1M Tris/HCl, pH7.4 1.8mL 0.5M Na <sub>2</sub> EDTA, pH8 1 bottle Proteinase inhibitor cocktail 10mL 10% Nonidet P40 solution 10mL Glycerin Add distilled water to a final volume of 100 mL
Laemmli buffer	8,34mL TrisHCL pH 6.8 5g SDS 0,25g bromothymolblue

## Material and methods

---

	25mL glycerol 3,45g DTT Add distilled water to a final volume of 50 mL
10x electrophoresis buffer	144g glycine 30g Tris 10g SDS Add distilled water to a final volume of 1 L
10x blotting buffer	30,28g Tris 106,6g glycine Add distilled water to a final volume of 1 L
1x blotting buffer	100 mL 10x blotting buffer 200 mL methanol Add distilled water to a final volume of 1 L
10x TBS	24 g Tris base 88 g NaCl pH to 7.4 with HCl Add distilled water to a final volume of 1 L
1x TBST	100 mL 10x TBS 500 µL Tween 20 Add distilled water to a final volume of 1 L
10% Formalin	25 mL Formaldehyde solution Add distilled water to a final volume of 250 mL
embryos/larave lysis buffer	133 µl of 1.5 M Tris/HCl, pH8 40 µl 0.5 M EDTA 60 µl Tween 60 µl Glycerol Add distilled water to a final volume of 20



## Material and methods

---

	mL
E3 (eggwater)	3 g Red Sea Salt Add distilled water to a final volume of 10 L
1-phenyl-2-thiourea (PTU, 10x stock)	304 mg PTU Add distilled water to a final volume of 10 L
Tris/HCl, pH 8/9	181.17 g Tris Adjust pH to 8/9 with HCl Add distilled water to a final volume of 1 L
0.1 M KCl	0.745 g KCl Add distilled water to a final volume of 100 mL
Tricaine (3-amino benzoic acidethylester)	400 mg Tricaine powder Adjust pH to 7 with Tris/HCl Add distilled water to a final volume of 100 mL
1% aqueous periodic acid	2 g periodic acid (H <sub>5</sub> JO <sub>3</sub> ) Add distilled water to a final volume of 200 mL
10% Sodium metasilphite	20 g Sodium metasilphite (Na <sub>2</sub> S <sub>2</sub> O <sub>5</sub> ) Add distilled water to a final volume of 200 mL
Hematoxylin (after Meyer)	1 g Hematoxylin 0.2 g Sodium iodate (NaIO <sub>3</sub> ) 50 g Potassium alum (KAl(SO <sub>4</sub> ) <sub>2</sub> *12 H <sub>2</sub> O) 50 g Chloral hydrate (C <sub>2</sub> H <sub>3</sub> Cl <sub>3</sub> O <sub>2</sub> )

## Material and methods

---

1 g Citric acid (C<sub>6</sub>H<sub>8</sub>O<sub>7</sub>)

Add distilled water to a final volume of 1 L

Sulfurous water

30 mL 1 M HCl

36 mL 10% Sodium metasilphite  
(Na<sub>2</sub>SiO<sub>3</sub>)

Add distilled water to a final volume of  
600 mL

### 2.1.5 Kits and Reagents

<b>Products</b>	<b>Company</b>
Alanine Assay Kit	Sigma-Aldrich
Biotin Switch Assay Kit (S-Nitrosylation)	abcam
DAB Peroxidase (HRP) Substrate Kit (with Nickel)	vector laboratories
Eukitt® Quick-hardening mounting medium	Sigma-Aldrich
Gene Ruler DNA ladder mix (0.5 µg/µl)	Thermo Fisher Scientific
Glutamate Assay Kit	Sigma-Aldrich
GoTaq® Green Master Mix	Promega
Maxima First Strand cDNA Synthesis Kit with dsDNase	molecular biology by thermo scientific
Power SYBR™ Green PCR Master Mix Kit	Applied Biosystems
QIAquick PCR Purification Kit	QIAGEN
RNeasy Mini Kit	QIAGEN
Tissue-Clear®	Tissue-Tek®, Sakura Finetek
Tricaine (3-amino benzoic acidethylester)	Sigma-Aldrich

### 2.1.6 Oligonucleotides

<b>CRISPR-construct name</b>	<b>Oligonucleotide sequence (5' to 3')</b>
<i>akr1a1b</i> -CRISPR#1-for	TAGGTCCAAGTACTCCAGCTTC
<i>akr1a1b</i> -CRISPR#1-rev	AAACGAAGCTGGAGTACTTGGA

<b>Genotyping primer name</b>	<b>Primer sequence (5' to 3')</b>
-------------------------------	-----------------------------------

## Material and methods

akr1a1b-genotyping#1-for	GGCGAGAGGATGTGTTTGTG
akr1a1b-genotyping#1-rev	GGGGCTCTATTATGGTCTTTTCA

gPCR gene name	Primer sequence
<i>akr1a1b</i>	CGTCTCTATTA AAAACTCTGAAAGACC AAGGGGTATCGCCTCGTT
<i>cpepck</i>	ATCACGCATCGCTAAAGAGG CCGCTGCGAAATACTTCTTC
<i>gls b</i>	GGATATGGAGCAGCGTGATT CTCATCCATTGGTGTGTTGC
<i>glud 1a</i>	CCGGTATAACCTTGGGCTGG CTCGGGTCTGCGTGGATAAG
<i>glut 1a</i>	TGACCGGCCCATACGTTTTTC ATCATCTCGGTTATATTTATCTGCC
<i>glut 2</i>	GCAGAAGAACCCTCACTC TCTCCGCCACAATAAACC
<i>sglt 1</i>	TGGAACGCTCTGGTTGTTGT TAGATGCGGATTCGCTGACC
<i>sglt 2</i>	ATGAGTCGGGTGCTTTCTGG ATGGCGCAGGGTAAAGACAA
<i>b2m</i>	ACTGCTGAAGAACGGACAGG GCAACGCTCTTTGTGAGGTG
<i>β-actin</i>	ACGGTCAGGTCATCACCATC TGGATACCGCAAGATTCCAT

### 2.1.7 Antibodies

Products	Company
Anti-Akr1a1b antibody(guinea pig) (For western blot, 1:1000 dilution) (For Immunohistochemistry , 1:100 dilution)	Keyhole Limpet Hemocyanin and DKFZ

Anti- $\beta$ -actin(rabbit)

(1:1000 dilution)

Cell Signaling Technology (4967S)

Anti-rabbit IgG, HRP-linked Antibody

(1:1000 dilution)

Cell Signaling Technology (7074S)

### 2.1.8 Zebrafish transgenic lines

Two transgenic zebrafish lines were used: *Tg(fli1:EGFP)* and *Tg(wt1b:EGFP)* for all the study of zebrafish (*Danio rerio*) experiments.

## 2.2 Methods

### 2.2.1 Animal studies

#### 2.2.1.1 Ethics

All experimental procedures on animals were approved by Medical Faculty Mannheim (license no.: I-19/01) and Regierungspräsidium Karlsruhe (license no. G-98/15) and carried out following the approved guidelines.

#### 2.2.1.2 Zebrafish maintenance

Both zebrafish lines were raised and staged as described according to hours post-fertilization (hpf). Embryos/larvae were kept in egg water at 28.5 °C with 0.003% 1-phenyl-2-thiourea (PTU, Sigma) to suppress pigmentation. Adult zebrafish were held under a 13 h light - 11 h dark cycle and fed with live shrimps and fish flake food.

#### 2.2.1.3 Incubation of zebrafish embryos/larvae

Fertilized eggs were incubated at 28.5 °C in 6-well plates with 5 mL solutions that was changed daily. The solution contained egg water, glutamate(0, 0.1 and 1 $\mu$ M), alanine(0, 1 and 5 $\mu$ M) and 0.003% PTU. Embryos were raised until 48hpf and analyzed for pronephric structure.

#### 2.2.1.4 Microscopy and analysis of pronephric alternations in larvae

For in vivo imaging of pronephric structures of embryos, 48 hpf *Tg(wt1b:EGFP)* embryos were anesthetized with a 0.003% tricaine and mounted in 1% low melting point agarose (Promega) dorsally. Images were taken by Leica DFC420 C camera, attached to a Leica

MZ10 F modular stereo microscope. Alterations of the pronephros were quantified by measuring the size of glomerular length, width, and neck length using Leica LAS V4.8 software.

### 2.2.1.5 Determination of pronephros function

After 72 hpf, 3 nl of Texas-Red® tagged 70 kDa dextran (2 mg/mL in PBS) was injected into the sinus venous of larvae. Images of living fish were taken sequentially at approximately 1, 24, and 48 hours post-injection (hpi) using an inverted microscope (Leica DMI 6000B) with a camera (Leica DFC420 C) and the Leica LAS application suite 3.8 software. NIH's ImageJ application was used to measure maximum fluorescence density in the heart area. The fluorescence values at 24hpi and 48hpi were divided by the fluorescence values of 1hpi; respectively, for each fish, the result was shown as a ratio of the fluorescence values.

### 2.2.1.6 Dissection of adult zebrafish

For kidney preparation, adult zebrafish were euthanized with 250 mg/L tricaine until the operculum movement stopped entirely. The fish were decapitated behind the operculum then transferred into pre-cooled 1 × PBS. Livers and kidneys, which remained in the body, were fixed in 10 % buffered formalin, routinely embedded in paraffin, and cut into 4 µm-thick sections for hematoxylin and eosin staining and for Periodic acid-Schiff reaction, partly in combination with diastase. Kidneys for EM study were fixed in 2% glutaraldehyde/0.01 M Na-cacodylate buffer and further processed according to protocols of the Electron Microscopy Core Facility of Heidelberg University.

### 2.2.1.7 Histology (Periodic acid-Schiff)

#### Dehydration of the tissue:

Day 1	70% Ethanol	2x 15 min
	70% Ethanol	overnight (4 °C)
Day 2	80% Ethanol	2x 15 min
	90% Ethanol	2x 15min
	96% Ethanol	3x 15min
	99% Ethanol	3x 15min
	Xylol	3x 5min (under the hood)

## Material and methods

---

	paraffin	1x 10 min (62°C)
	paraffin	overnight (62°C)
Day 3	relocated tissue	until entirely cooled

### Periodic acid-Schiff staining:

Tissue Clear	2x 10 min
99% Ethanol	1x 5 min
96% Ethanol	1x 5 min
70% Ethanol	1x 5 min
Distilled water	2x 5 min
1% Periodic acid	1x 10 min
Distilled water	Rinsing
Schiff's reagent	1x 20 min
Sulfurous water	3x 2 min
Running water	1x 5 min
Hematoxylin	1x 5 min
running water	1x 5 min
70% Ethanol	1x 5 min
99% Ethanol	3x 1 min
Tissue clear	3x 1 min
Acetic acid n-butyl ester	store until covered

Then the sections were covered with cover-glasses where Eukitt® Quick-hardening mounting medium was applied on and left under the hood until the mounting medium was solidified properly. Slides were analyzed with.

#### *2.2.1.8 Measurement of adult zebrafish blood glucose*

Adult zebrafish were transferred to single boxes the day before. The next day, the fish were either directly euthanized for blood sugar measurements under overnight fasting conditions or fed with 0.5g flake food for postprandial conditions. After feeding, the zebrafish were euthanized in 250 mg/L tricaine, and blood glucose was measured.

## Material and methods

---

### 2.2.2 Molecular biology

#### 2.2.2.1 Isolation of genomic DNA

Zebrafish embryos/larvae or cut fins of adult zebrafish were collected into 0.2 mL Eppendorf tubes each, 20  $\mu$ L lysis- buffer was added and the tubes placed in a PCR cyclor operated as follow:

98 °C 10 min

Add 10  $\mu$ L proteinase K (of the 10 mg/mL stock)

55 °C for at least 4 h or overnight

Mix samples by flicking the tubes until embryos/fins are nearly dissolved entirely

55 °C 1 h

98 °C 10 min

Mix carefully and centrifuge briefly (genomic DNA ready to use for PCR)

#### 2.2.2.2 Polymerase chain reaction (PCR)

For the genotyping of mutant, the primer(see 2.1.6, Genotyping primer) was designed by the previous colleague in our group. And the PCR technology was used:

#### PCR reaction system:

	<u>25 <math>\mu</math>L</u>
genomic DNA	2 $\mu$ L
forward primer	1.5 $\mu$ L
reverse primer	1.5 $\mu$ L
GoTaq® Green Master Mix	12.5 $\mu$ L
distilled water	7.5 $\mu$ L

#### PCR program:

step 1	95 °C	3 min
step 2	95 °C	30 sec
	60 °C	30 sec
	72 °C	30 sec
	35 cycels for step 2	
step 3	72 °C	5 min
	4°C	( $\infty$ )

### 2.2.2.3 DNA gel electrophoresis

3% agarose gel was performed for the DNA fragments separation, the gel was run at 120 V (100 mL gel) in 0.5x TAE for 2 hours.

### 2.2.2.4 RNA isolation from larvae and adult zebrafish organs.

Early developmental stages of zebrafish from 24 hpf to 120 hpf were anesthetized with 0.003% tricaine and collected into 1.5 mL Eppendorf tubes, 20 embryos/ larvae each. Then the samples were snap frozen in liquid nitrogen and used for RNA isolation immediately or stored at -80 °C freezer. Adult zebrafish organs, heart, spleen, liver, kidney, eyes, brain, and muscle, were collected during fish dissection and snap frozen in liquid nitrogen used for RNA isolation immediately or stored at -80 °C freezer.

Lysis and isolation of RNA of the embryos/larvae or adult zebrafish organs were performed with the RNeasy Mini Kit (Qiagen) according to the manufacturer's protocol. RNA concentration was measured with the photometer, and integrity was checked on 1% agarose gel. Then samples were stored at -80 °C until use.

### 2.2.2.5 cDNA synthesis from RNA (RT-PCR)

Reverse transcription PCR (RT-PCR) from RNA of the embryos/larvae or adult zebrafish organs was performed using the Maxima First Strand cDNA Synthesis Kit. All steps were carried out according to the manufacturer's protocol in which 1 µg RNA was utilized as the template. After all, the cDNA was appropriately diluted and stored at -20 °C.

### 2.2.2.6 Real-time quantitative PCR (RT-qPCR)

All primers (see 2.1.6, qPCR gene) were designed with the Primer-BLAST tool of NCBI (<https://www.ncbi.nlm.nih.gov/>). Among these, *β-Actin* and *b2m* were used as references. Power SYBR™ Green PCR Master Mix Kit was used for the reaction, which performed with QuantStudio 3 Real-Time-PCR-System as below:

#### qPCR reaction system:

	<u>10 µL</u>
cDNA	1 µL
primer mix(including forward primer and reverse primer)	1 µL



## Material and methods

---

SYBR	5 $\mu$ L
distilled water	3 $\mu$ L

### qPCR program:

step 1	95 °C	3 min
step 2	95 °C	15 sec
	60 °C	30 sec
	40 cycles for step 2	

### *2.2.2.7 Western blot analysis*

Western blot technology was used for identifying the establishment of akr1a1b knock-out model and S-nitrosylation levels in the mutants.

For analysis of Akr1a1b expression, 1-year-old adult zebrafish livers were taken and lysed in NP40 lysis buffer (150mmol/L NaCl, 50mmol/L Tris-HCl, pH7.4, 1% NP40, 10mmol/L EDTA, 10% glycerol, and protease inhibitors), followed by homogenization with a syringe and incubation on ice for 30min on a shaker. The supernatant containing the protein lysate was diluted 5:1 with Laemmli sample buffer and boiled at 95°C for 5 min, separated via SDS-PAGE, and then transferred to a nitrocellulose membrane for antibody incubation (anti-Akr 1A1b antibody 1:1000, anti-Actin antibody(A2228, Sigma-Aldrich) 1:1000, secondary antibody 1:1000( $\beta$ -actin: rabbit anti-goat, P0160, Dako; Akr1a1b: goat anti-guinea pig, ABIN101281, antibodies-online.com). Visualization by enhanced chemiluminescence (ECL) was acquired after incubation with HRP (Horseradish Peroxidase) substrate.

S-Nitrosylation was isolated by using the Biotin Switch Assay Kit (Abcam, ab236207), with a modification of the “Biotin-Switch” method, according to the manufacturer’s instructions to measure S-nitrosylated (S-NO) proteins in adult liver lysates.

### *2.2.2.8 Immunohistochemistry*

Kidney tissue from wild-type zebrafish was used for the analysis of Akr1a1b protein expression. The experiment was performed on 4  $\mu$ m paraffin-embedded tissue sections fixed in 4% paraformaldehyde (PFA). The sections were dewaxed, rehydrated, antigen retrieved by boiling sections in 0.01 M sodium citrate buffer (pH 6.0) in 480 W microwave for 20min, followed by removal of endogenous peroxidase activity by a 3% solution of H<sub>2</sub>O<sub>2</sub>/methanol for 20 min, nonspecific antibody binding was blocked by

incubation with 10% FBS/PBS for 1 hour. The primary antibody diluted in 10% FBS/PBS was applied overnight at 4°C. Afterward, sections were washed three times in PBS and then incubated in a 1:1000 diluted secondary antibody for 30min at room temperature. Diaminobenzidine (DAB, SK-4100, vector laboratories) was used for chromogens for HRP and counterstained by Hematoxylin. Then all sections were dehydrated and sealed for analysis. For Akr1a1b antibody generation, peptide AWKHPDEPVLLLEPAIAAL-C was synthesized and coupled to KLH (Keyhole Limpet Hemocyanin) by PSL GmbH, Heidelberg, Germany and subsequently injected into guinea pigs for immunization following standard procedures from CF Unit Antibodies, DKFZ Heidelberg, Germany.

### 2.2.3 Biochemical analysis

#### 2.2.3.1 *Determination of activity of Akr, ALDH and Glo1 enzymes*

Akr activity was determined spectrophotometrically by measuring the rate of reduction of NADPH at 340 nm at pH7.0 at 25°C. The assay mixture contained 100mM potassium phosphate, 0.1–2 mM methylglyoxal (MG) and 0.1mM NADPH. One unit of enzyme activity is defined as the amount of the enzyme required to oxidize 1  $\mu$ mol of NADPH/min. Glo1 (Glyoxalase 1) activity measurement was based upon the formation of S-D-lactoylglutathione from the hemithioacetal substrate, prepared from the pre-incubation of 50mM sodium phosphate (pH6.6), 2mM methylglyoxal and 2mM reduced GSH, and was determined spectrophotometrically by measuring the increase in absorbance at 235 nm at pH 6.6 at 25°C. ALDH activity was assayed at 25°C in 75 mM Tris-HCl (pH 7.6) containing 10 mM BSA, 0.5 mM NADP, and 0.1–2 mM MG.

#### 2.2.3.2 *Determination of methylglyoxal (MG), 3-Deoxyglucosone (3-DG), and glyoxal*

MG, 3-DG, and glyoxal levels of zebrafish larvae, whole body lysates, and eyes were determined by LC-MS/MS, as described previously. Tissue MG levels were determined by derivatization with 1,2-diaminobenzene (DB). Briefly, pre-weighed amounts of tissue (ca.10 mg) were homogenized in ice-cold 20% (wt/vol) trichloroacetic acid in 0.9% (wt/vol) sodium chloride (20  $\mu$ L) and water (80  $\mu$ L). An aliquot (5  $\mu$ L) of the internal standard ( $^{13}\text{C}_3$ -MG; 400 nM) was then added, and the samples mixed. Following centrifugation (20,817 g; 5 minutes at 4°C), 35  $\mu$ L of the supernatant was transferred to an HPLC vial containing a 200- $\mu$ L glass insert. An aliquot (5  $\mu$ L) of 3% sodium azide

(wt/vol) was then added to each sample, followed by 10  $\mu$ L of 0.5 mM DB in 200 mM HCl containing 0.5 mM diethylenetriaminepentaacetic acid (DETAPAC) in water. The samples were then incubated for 4 hours at room temperature, protected from the light. Samples were then analyzed by LC-MS/MS using an ACQUITY ultra-high-performance liquid chromatography system with a Xevo-TQS LC-MS/MS mass spectrometer (Waters). The columns were a Waters BEH C18 (100  $\times$  2.1 mm) and a guard column (5  $\times$  2.1 mm). The mobile phase was 0.1% formic acid in water with a linear gradient of 0% to 100% 0.1% formic acid in 50% acetonitrile/water over 0 to 10 minutes; the flow rate was 0.2 mL/min and the column temperature was 5°C. The capillary voltage was 0.5 kV, the cone voltage 20 V, the interscan delay time 100 ms, the source and desolvation gas temperatures 150°C and 350°C, respectively, and the cone gas and desolvation gas flows were 150 and 800 L/h, respectively. Mass transitions (parent ion  $\rightarrow$  fragment ion; collision energy), retention time, the limit of detection, and recoveries were as follows: 145.0  $\rightarrow$  77.1, 24eV, 5.93 minutes, 0.52 pmol, and 98%.

### 2.2.3.3 *Metabolomic analysis*

Detection was done in cooperation with the Metabolomics Core Technology Platform from the Centre of Organismal Studies Heidelberg. At 96 hpf, zebrafish larvae were anesthetized with 0.003% tricaine, collected, and snap-frozen in liquid nitrogen. Metabolites were determined via semi-targeted gas chromatography-mass spectrometry (GC/MS) analysis and ultra-performance liquid chromatography with fluorescence detection (UPLC-FLR) analysis (67). Frozen, ground sample material from zebrafish was extracted in 360  $\mu$ L of 100% MeOH for 15 minutes at 70°C with vigorous shaking. As internal standards, 20  $\mu$ L ribitol (0.2 mg/mL) and 10  $\mu$ L heptadecanoic acid (0.2 mg/mL) were added to each sample. After the addition of 200  $\mu$ L chloroform, samples were shaken at 37°C for 5 minutes. To separate polar and organic phases, 400  $\mu$ L water was added, and samples were centrifuged for 10 minutes at 11,000  $\times$  g. For the derivatization, 700  $\mu$ L of the polar (upper) phase were transferred to a fresh tube and dried in a speed-vac (vacuum concentrator) without heating. Pellets of the aqueous phase after extraction were re-dissolved in 20  $\mu$ L methoximation reagent containing 20 mg/mL methoxyamine hydrochloride (Sigma-Aldrich 226904) in pyridine (Sigma-Aldrich 270970) and incubated for 2 hours at 37°C with shaking. For silylation, 32.2  $\mu$ L N-

## Material and methods

---

methyl-N-(trimethylsilyl)trifluoroacetamide (MSTFA; Sigma M7891) and 2.8  $\mu$ L Alkane Standard Mixture (50 mg/mL C10–C40; Fluka 68281) were added to each sample. After incubation for 30 minutes at 37°C, samples were transferred to glass vials for GC/MS analysis. To analyze total fatty acids, 150  $\mu$ L of the lower organic phase (chloroform) after extraction were transferred to a fresh 1.5-mL reaction tube and dried in a speed-vac without heating. For transmethylation reactions, pellets were re-dissolved in 40  $\mu$ L TBME (tert-butyl methyl ether, Sigma-Aldrich) and 20  $\mu$ L TMSH (trimethylsulfoniumhydroxid, Sigma-Aldrich), incubated for 45 minutes at 50°C, and transferred to glass vials for GC/MS analysis of the fatty acid methyl esters (FAMES). A GC/MS-QP2010 Plus (Shimadzu) fitted with a Zebron ZB 5MS column (Phenomenex; 30 meter  $\times$  0.25 mm  $\times$  0.25  $\mu$ m) was used for GC/MS analysis. The GC was operated with an injection temperature of 230°C and a 1- $\mu$ L sample was injected with split mode (1:10). The GC temperature program started with a 1-minute hold at 40°C followed by a 6°C/min ramp to 210°C, a 20°C/min ramp to 330°C, and a bake-out for 5 minutes at 330°C using Helium as carrier gas with constant linear velocity. The MS was operated with ion source and interface temperatures of 250°C, a solvent cut time of 7 minutes, and a scan range (m/z) of 40 to 700 with an event time of 0.2 s. The “GCMS solution” software (Shimadzu) was used for data processing.

### 2.2.3.4 Measurement of glutamate and alanine in adult zebrafish kidneys and livers

Glutamate and alanine concentration was measured using the Glutamate Assay Kit (MAK004, Sigma-Aldrich) and Alanine Assay Kit (MAK001, Sigma-Aldrich) according to the manufacturer's instructions, and represented as ng/mg tissue.

### 2.2.4 Statistical analysis

All data are presented as mean  $\pm$  SD. Statistical significance between two groups was analyzed using two-tailed Student's *t*-test using GraphPad Prism, For comparisons among more than two groups, one-way or two-way ANOVA followed by appropriate multiple comparison tests was used. *P* value less than 0.05 was considered significant.



Previous studies showed *akr1a1* expression in virtually every tissue in humans and mice, with being highest expressed in the kidney tubular system<sup>(Fagerberg et al., 2014; Scotcher et al., 2016; Yue et al., 2014)</sup>. Yet, the expression of *akr1a1b* in zebrafish has not been analyzed. Thus, I investigated early developmental stages from 24 hpf to 120 hpf, and organs from adult zebrafish for *akr1a1b* expression using quantitative RT-PCR. Results showed that *akr1a1b* was abundantly expressed throughout embryonic and larval stages (Fig. 5a) and also in all analyzed adult organs with being highest expressed in livers (Fig. 5b). Since mouse *akr1a1* is highly expressed in the kidney tubular system<sup>(Zhou et al., 2019)</sup>, I assessed *Akr1a1b* expression in adult zebrafish kidneys by immunohistochemical staining, and demonstrated a similar localization in the tubular system as described in mice (Fig. 5c).

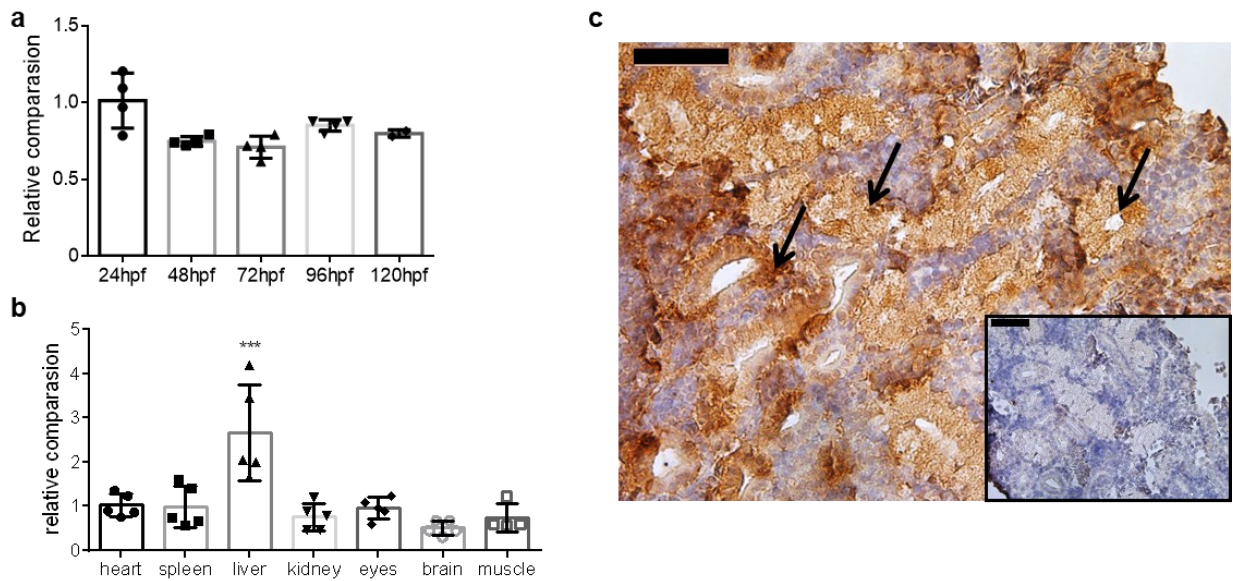


**Figure 5: Expression of *akr1a1b* gene in zebrafish development and in adult organs**

**a)** *Akr1a1b* is ubiquitously expressed in zebrafish development (relatively compared with 24hpf,  $n = 4$ , mean  $\pm$  SD) and **(b)** in all analyzed organs of adult zebrafish (relatively compared with heart,  $n = 5$ , mean  $\pm$  SD). **(c)** In adult zebrafish kidney, immunohistochemistry revealed high *Akr1a1b* expression in renal tubules (arrows). Box shows kidney immunostaining with secondary antibody only. Expression of genes in A and B was determined by RT-qPCR and normalized to  $\beta$ -actin. \*\*\*  $p < 0.001$ ,  $p$  value was calculated by one-way ANOVA. Scale bars in C: 50  $\mu$ m.

## Result

### 3.2 Generation and validation of *akr1a1b*<sup>-/-</sup> mutants

To address the physiological role of *akr1a1b* in zebrafish development and physiology, we have established a permanent knockout zebrafish model using CRISPR-Cas9 technology. Following the injection of the gRNA together with Cas9 RNA targeted at exon 4 of zebrafish *akr1a1b* gene(Fig. 6a), two different frame-shift mutants were identified and used for the subsequent studies, including a 17 base-pair insertion in the *tg(wt1b:EGFP)* reporter line and a 23 base-pair deletion in the *tg(fli1:EGFP)* reporter line(Fig. 6b).

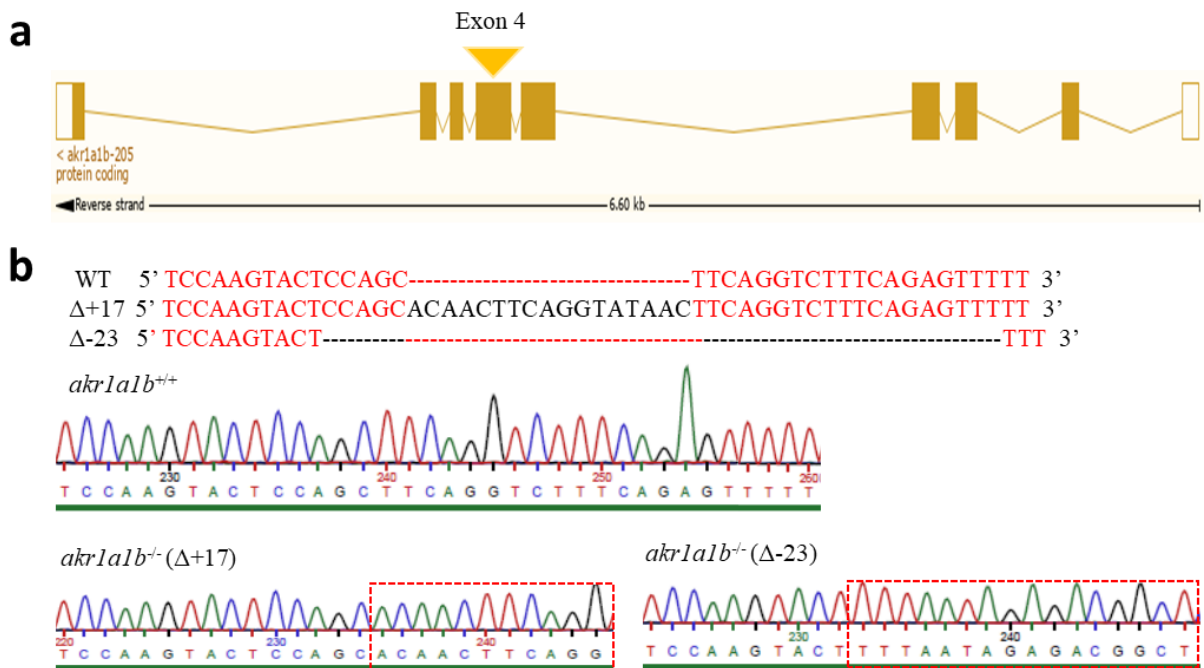


**Figure 6: Generation of *akr1a1b*<sup>-/-</sup> zebrafish mutants**

(a) Schematic depiction of the *akr1a1b* gene, which highlights exon 4 as CRISPR-Cas9 target site([https://www.ensembl.org/Danio\\_rerio/Transcript/Summary?db=core;g=ENSDARG00000052030;r=6:33918813-33925432;t=ENSDART00000145019](https://www.ensembl.org/Danio_rerio/Transcript/Summary?db=core;g=ENSDARG00000052030;r=6:33918813-33925432;t=ENSDART00000145019)). (b) CRISPR-Cas9 technology was used to establish *akr1a1b* knock-out zebrafish. Schematic depiction of wildtype *akr1a1b* target sequence and two identified frameshift mutations and their corresponding chromatograms including a 17 base-pair insertion and a 23 base-pair deletion. Red dashed boxes indicate start of genomic alterations.

## Result

Western blot technology was then used to confirm the loss of Akr1a1b in the mutants. The result showed that Akr1a1b protein expression in adult livers was utterly abolished in both mutants (Fig. 7a). In addition, the enzyme activity was significantly decreased in *akr1a1b*<sup>-/-</sup> larvae (Fig. 7b).

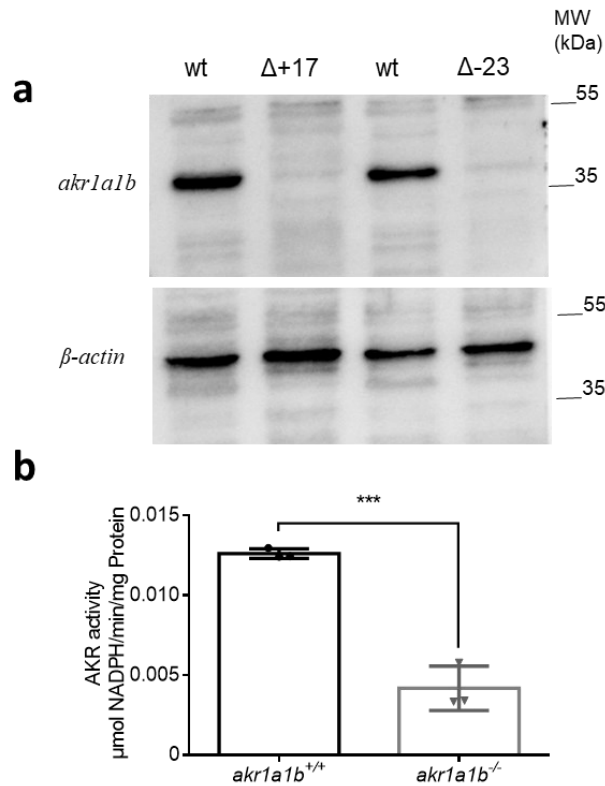


**Figure 7: Validation of *akr1a1b*<sup>-/-</sup> zebrafish mutants**

(a) Western blot for Akr1a1b expression in zebrafish livers showed absent of Akr1a1b protein in the 17 base-pair insertion and in the 23 base-pair deletion mutant, respectively, which validates the *akr1a1b* knock-out zebrafish model. (b) In addition, *akr1a1b*<sup>-/-</sup> zebrafish larvae at 96 hpf showed a strong descend of AKR enzyme activity. \*\*\* $p < 0.0001$ .



## Result

After confirming the knockout of *akr1a1b* in zebrafish, internal AGEs precursors, including methylglyoxal (MG), glyoxal and 3-deoxyglucosone (3-DG) levels, were measured to evaluate the importance of Akr1a1b for the detoxification of reactive metabolites in zebrafish. Interestingly, concentration of the dicarbonyl methylglyoxal (MG) (Fig. 8a), but not of 3-Deoxyglucosone (3-DG), and glyoxal (Fig. 8b, c) as reactive metabolites leading to advanced glycation end-products (AGEs), was significantly increased in *akr1a1b*<sup>-/-</sup> larvae at 96 hpf. Together, the data have proven a successful generation and validation of *akr1a1b* mutant zebrafish, which only shows an increase for MG.

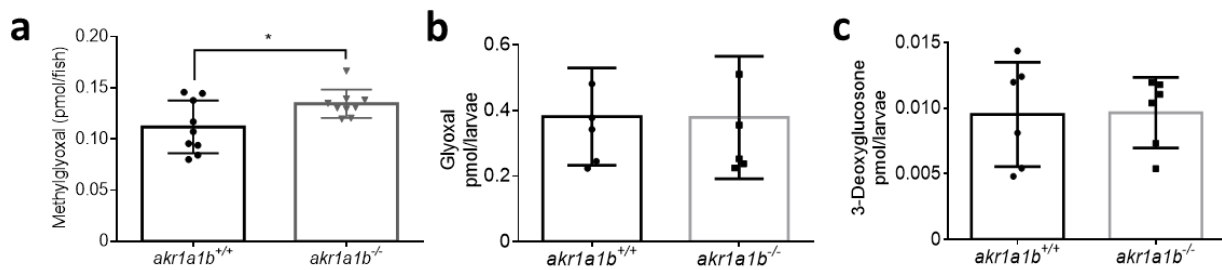


**Figure 8: AGEs precursors levels in *akr1a1b*<sup>-/-</sup> zebrafish mutants**

(a, b, c) *Akr1a1b*<sup>-/-</sup> larvae at 96 hpf showed increased MG concentrations (n = 9 clutches with 50 larvae); meanwhile Glyoxal and 3-Deoxyglucosone were not, as determined by LC-MS/MS (n = 6 clutches with 50 larvae). \**p* < 0.05.

### 3.3 *Akr1a1b* knock-out in zebrafish caused alterations of the embryonic pronephros and of adult kidneys

Since Akr1a1b is prominently expressed in zebrafish renal tubules (Fig. 5c), we hypothesized a significant effect for *akr1a1b* knockout on kidney development and kidney function in zebrafish. The zebrafish pronephros starts to develop at 16 hpf and reaches its full functionality at 96 hpf<sup>(Drummond and Davidson, 2010)</sup>. Structurally, at 48 hpf, the zebrafish pronephros is simply composed of two nephrons and functionally consist of two blood-filtering glomeruli, although leaky at this time, two proximal and distal tubules, and the pronephric duct (Fig. 9a). In the morphological analysis in *Tg(wt1b:EGFP)* line, which shows a pronephros-specific GFP-expression, labelling the glomerulus, the neck and the tubular structures that together form the pronephros, compared with the

## Result

*akr1a1b*<sup>+/+</sup> embryos at 48 hpf, *akr1a1b*<sup>-/-</sup> embryos displayed an enlarged glomerulus, where the length was substantially increased from  $88.6 \pm 10.8 \mu\text{m}$  in the *akr1a1b*<sup>+/+</sup> to  $106.3 \pm 19.1 \mu\text{m}$  in *akr1a1b*<sup>-/-</sup> mutants. The pronephric neck was significantly shortened to  $74.9 \pm 19.3 \mu\text{m}$  in *akr1a1b*<sup>-/-</sup> embryos compared with  $97.9 \pm 14.6 \mu\text{m}$  in the *akr1a1b*<sup>+/+</sup> group (Fig. 9b, c).

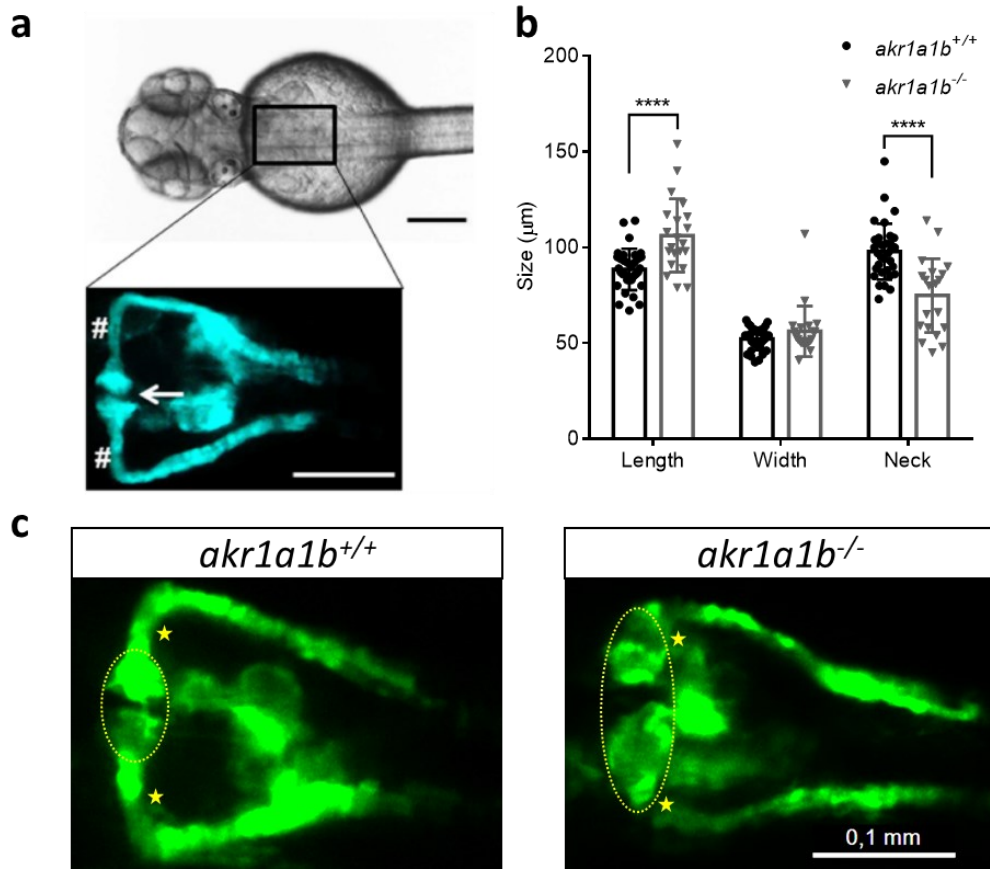


**Figure 9: *Akr1a1b* knock-out in zebrafish caused alterations of the embryonic pronephros**

(a) Illustrates the position of the pronephros in a *Tg(wt1b:EGFP)* embryo (48 hpf), visible from the dorsal view. The renal structure is composed of two tubules that are fused to form a single glomerulus (white arrow) via a neck (white hashtag). (b,c ) Compared with *akr1a1b*<sup>+/+</sup> embryos (n=33, mean ± SD) at 48 hpf, *akr1a1b*<sup>-/-</sup> mutants (n=21, mean ± SD) displayed an enlarged glomerulus (encircled) and shorten tubular neck (asterisk). \*\*\*\*  $p < 0.0001$ . Scale bar: 0.1 mm.

Furthermore, to evaluate whether renal functionality was affected by the *akr1a1b* knockout, I assessed the pronephric ultrafiltration in zebrafish larvae. Upon sinus venous injection of the 70 kDa Texas-Red® dextran (Fig. 10a), a significantly increased

## Result

loss of fluorescence in *akr1a1b*<sup>-/-</sup> (the ratios are  $0.516 \pm 0.079$  and  $0.364 \pm 0.079$  at 24 hpi and 48 hpi, respectively) compared to the *akr1a1b*<sup>+/+</sup> larvae (the ratios are  $0.621 \pm 0.090$  and  $0.427 \pm 0.076$  at 24 hpi and 48 hpi, respectively) was observed (Fig. 10b, c, d). This indicates adversity in the ultrafiltration in the *akr1a1b*<sup>-/-</sup> larvae.

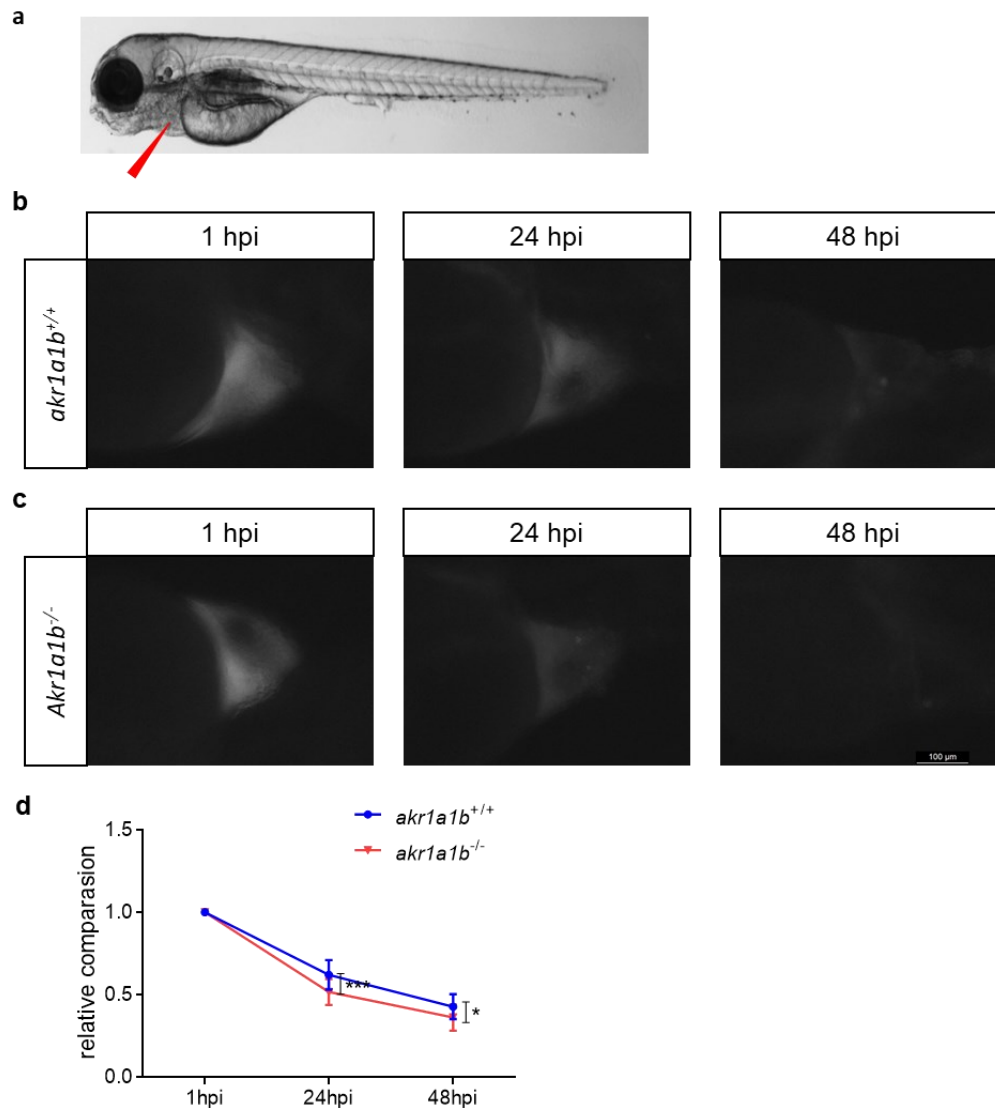


**Fig. 10 Measurement of heart fluorescence over time for the pronephric functional assesment in zebrafish.**

(a) Indicates the location where Texas Red® tagged 70 kDa dextran was injected into. (b, c) Images were taken at 1 hpi, 24 hpi and 48 hpi and the relative fluorescence in the heart region of *akr1a1b*<sup>+/+</sup> zebrafish larvae and *akr1a1b*<sup>-/-</sup> zebrafish larvae was measured using imageJ. Scale bar: 100  $\mu$ m. (d) A significant increased loss of fluorescence in *akr1a1b*<sup>-/-</sup> mutants (n=18, mean  $\pm$  SD) was observed as compared to *akr1a1b*<sup>+/+</sup> larvae (n=21, mean  $\pm$  SD). \*  $p < 0.05$ , \*\*\*  $p < 0.001$ . hpi: hours post injection

## Result

Thus, all the results above indicated that *akt1a1b* deficiency altered not only the pronephric structure but also the renal functionality in the early stage of zebrafish.

Based on the findings in *akt1a1b*<sup>-/-</sup> embryos/larvae, we performed a histological and electron microscopy analysis of adult *akt1a1b*<sup>-/-</sup> kidneys to address whether the pronephros developmental impairments in embryos/larvae persisted into adult zebrafish. In most adult *akt1a1b*<sup>-/-</sup> kidneys, a deposition of diastase-resistant PAS-positive hyaline droplets, putatively lysosomes, with a mild to a moderate amount and a small to medium size within the epithelium of proximal tubules were found (Fig. 11a, 12a). In contrast, the kidneys of *akt1a1b*<sup>+/+</sup> animals only have scattered small droplets (Fig. 11a, 12a), which were valued as a physiological finding as known from other animal species<sup>(Decker et al., 2012; Sato et al., 2005)</sup>. Furthermore, electron microscopy analysis showed *akt1a1b* deficiency zebrafish developed a strongly and significantly thicker glomerular membrane (Fig. 12b,c).

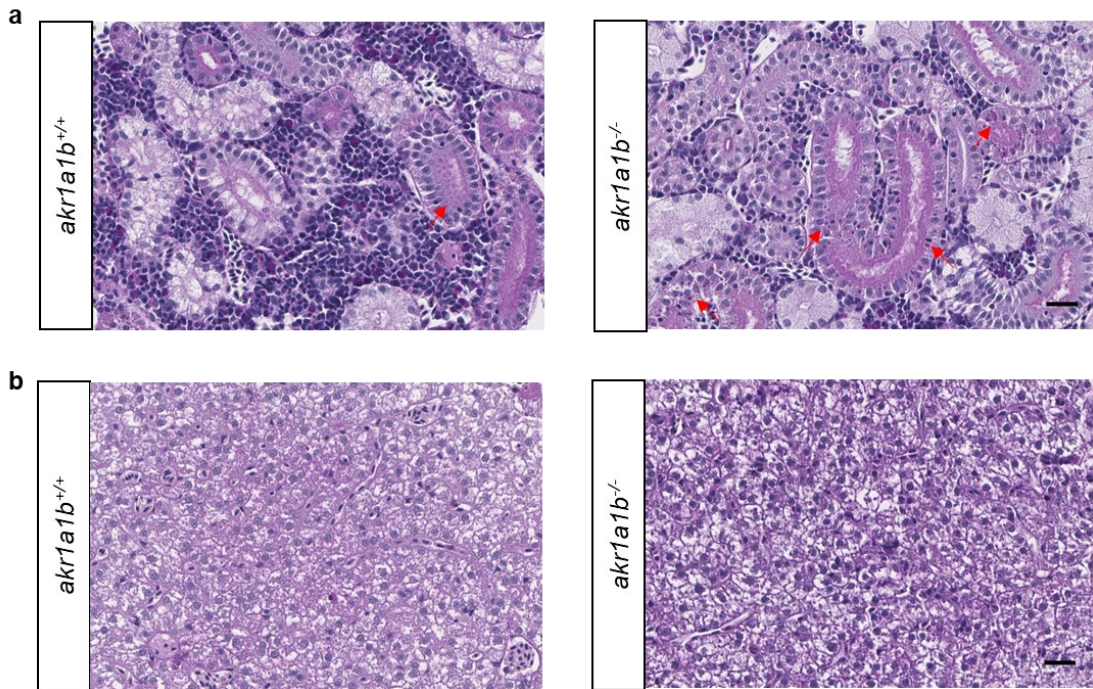


**Figure 11: *Akr1a1b* knockout altered adult zebrafish kidneys, but livers remained normal**

**(a)** Periodic acid–Schiff (PAS) staining showed deposition of diastase-resistant PAS-positive hyaline droplets, putatively lysosomes (red arrows), within the epithelium of proximal tubules. *Akr1a1b*<sup>+/+</sup> kidneys only have scattered small droplets. **(b)** Adult *akt1a1b*<sup>-/-</sup> livers stained by PAS were unaltered. Scale bars: 20  $\mu$ m.



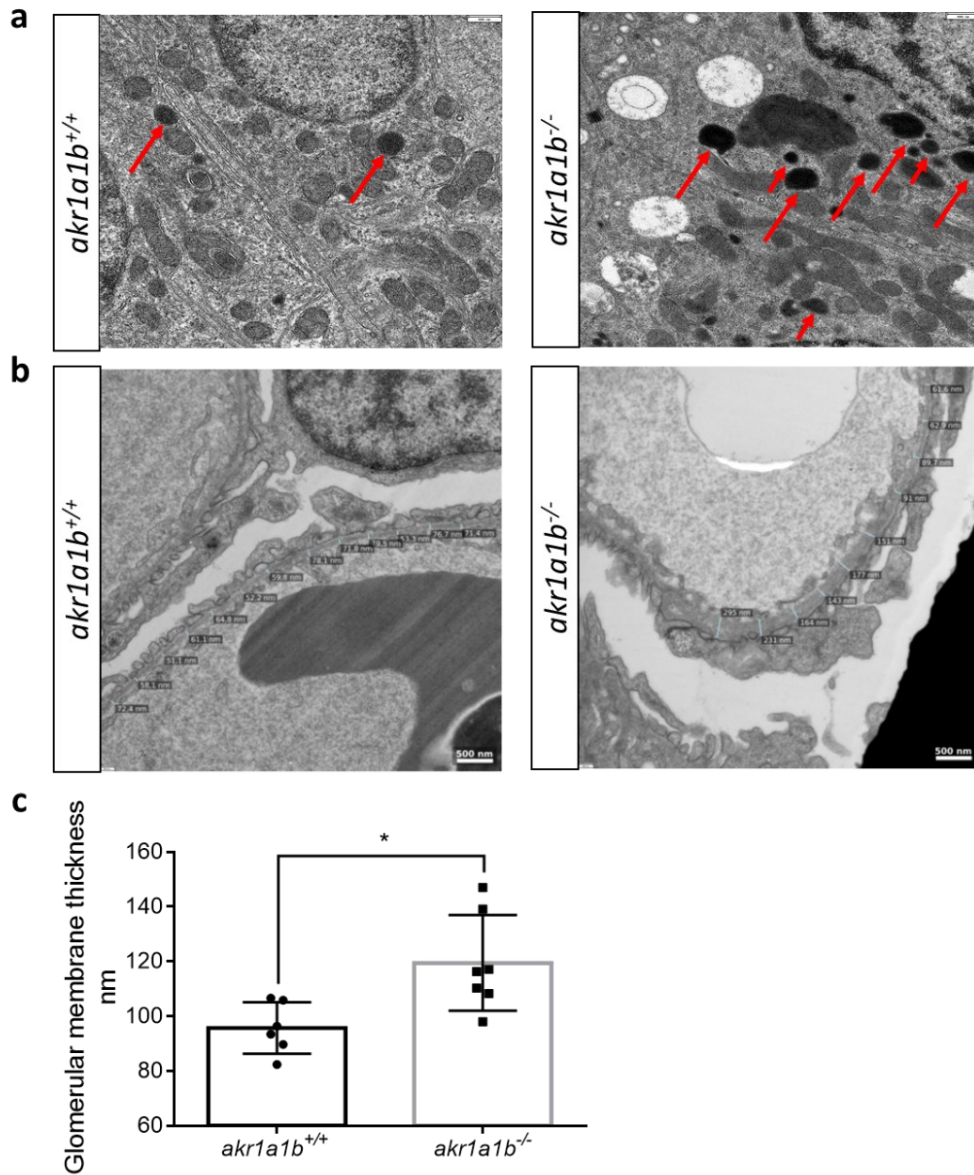


**Figure 12: *Akr1a1b* knockout altered adult zebrafish renal tubular and glomerular membrane**

(a) electron microscopy showed deposition of droplets, putatively lysosomes (red arrows), within the epithelium of proximal tubules. *Akr1a1*<sup>+/+</sup> kidneys only have scattered small droplets. (b,c) Adult *akr1a1b*<sup>-/-</sup> kidney showed significant thicker of glomerular membrane. Scale bars: 500 nm.

Since livers showed highest *akr1a1b* expression (Fig. 5b), we also analyzed the histology of adult *akr1a1b*<sup>-/-</sup> livers (Fig. 11b). Yet, overall morphology was not altered in this organ. Taken together, knockout of *akr1a1b* in zebrafish altered the embryonic pronephros and adult kidney, but other organs, including the liver, appeared normal.

## Result

### 3.4 Glutamate accumulated in *akr1a1b*<sup>-/-</sup> zebrafish and caused pronephros alterations

To investigate the underlying mechanisms of the pronephric and renal abnormalities, we performed metabolic profiling, including analysis of several amino acids, fatty acids, adenosines, and a set of primary metabolites in *akr1a1b*<sup>+/+</sup> and *akr1a1b*<sup>-/-</sup> zebrafish larvae at 96 hpf. The result showed a minor alteration of several amino acids and adenosine, like Ile, Leu, Phe, Pro, Trp (Fig. 13a), and NADH (Fig. 13b), but no significant difference of all fatty acids (Fig. 13c) between *akr1a1b*<sup>+/+</sup> and *akr1a1b*<sup>-/-</sup> zebrafish larvae.

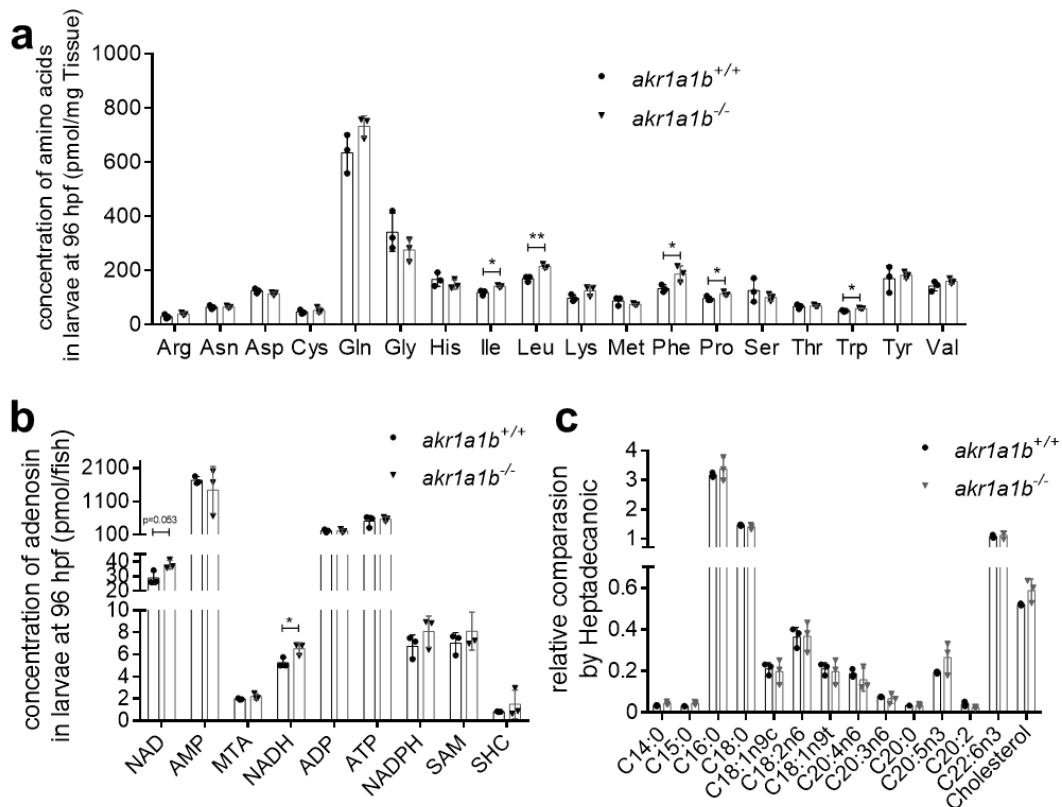


**Figure 13: *Akr1a1b* knock-out caused minor altered of amino acids and adenosine in 96hpf larvae**

Amino acids, adenosine and fatty acids were measured in 96 hpf old larvae by UPLC-MS/MS (n = 3 clutches with 50 larvae, mean ± SD) (a) Amino acids showed a minor altered profile in *akr1a1b*<sup>-/-</sup> larvae, in which Ile, Leu, Phe and Trp were slightly but significant increase; meanwhile all other amino acids didn't affect by *akr1a1b* deficiency. (b) Only NADH of adenosine profile showed a significant increase in *akr1a1b* deficiency larvae. (c) all fatty acids showed no alteration between each group. \*p<0.05, \*\*p<0.01

## Result

Although most primary metabolites were not significantly changed (Fig. 14a), lactic acid and malic acid were slightly increased (Fig. 14a), and citric acid and 2-keto glutaric acid showed a significant increased concentration (Fig. 14b), indicating a dysfunctional glucose metabolism. Yet, interestingly, we found increased concentrations of two glucogenic metabolites, namely glutamate and alanine in *akr1a1b*<sup>-/-</sup> zebrafish larvae at 96 hpf (Fig. 14c).

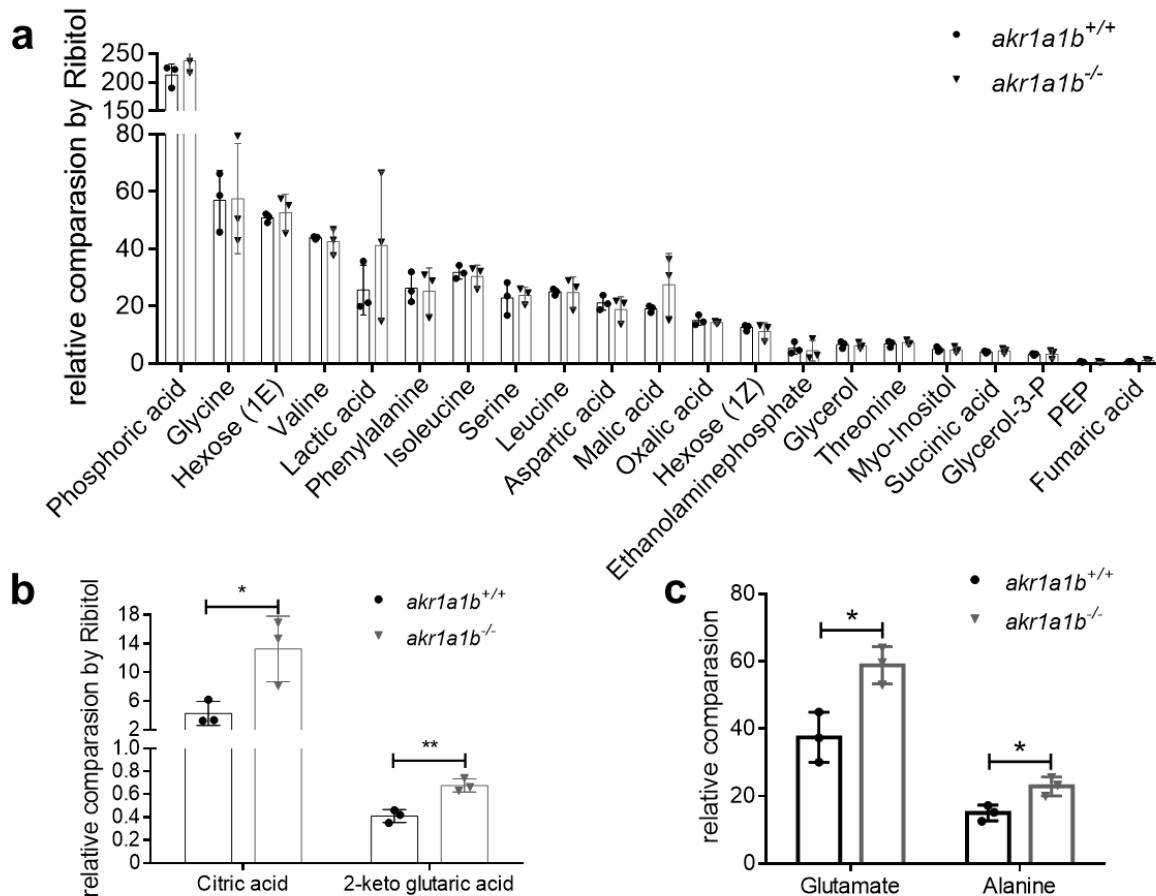


**Figure 14: *Akr1a1b* knock-out caused alterations of several primary metabolites in 96hpf larvae**

All primary metabolites were measured in 96 hpf old larvae by GC-MS (n = 3 clutches with 50 larvae, mean ± SD). (a) Most primary metabolites were not significantly changed. (b) citric acid and 2-keto glutaric acid were significant increased in *akr1a1b*<sup>-/-</sup> zebrafish larvae. (c) two glucogenic metabolites, glutamate and alanine, were significant increased in *akr1a1b*<sup>-/-</sup> zebrafish larvae. \*p<0.05, \*\*p<0.01

## Result

To test the hypothesis that elevated concentrations of glutamate and alanine may cause the observed pronephros phenotype in *akr1a1b*<sup>-/-</sup> mutants (Fig. 9, 10), *tg(wt1b:EGFP)* embryos were incubated for 48 hours in increasing concentrations of glutamate and alanine containing medium, and subsequently, the pronephros was analyzed. In zebrafish treated with 0.1 mM and 1 mM glutamate, the glomerular length was increased to  $89.6 \pm 10.9 \mu\text{m}$  and  $91.8 \pm 9.8 \mu\text{m}$ , respectively, while it was  $82.6 \pm 9.1 \mu\text{m}$  in egg water. The pronephric neck was shortened to  $100.3 \pm 14.5 \mu\text{m}$  and  $88.8 \pm 15.5 \mu\text{m}$ , respectively, while it was  $111.3 \pm 12.6 \mu\text{m}$  in egg water (Fig. 15a, b). In wild type zebrafish larvae treated with 1 mM glutamate and subsequent 70 kDa Texas-Red® dextran injection, significantly increased loss of fluorescence was observed both at 24 hpi and 48 hpi (the ratios are  $0.513 \pm 0.084$  and  $0.350 \pm 0.052$  at 24 hpi and 48 hpi, respectively), compared to larvae treated with egg water (the ratios are  $0.620 \pm 0.107$  and  $0.432 \pm 0.052$  at 24 hpi and 48 hpi, respectively) (Fig. 15c).

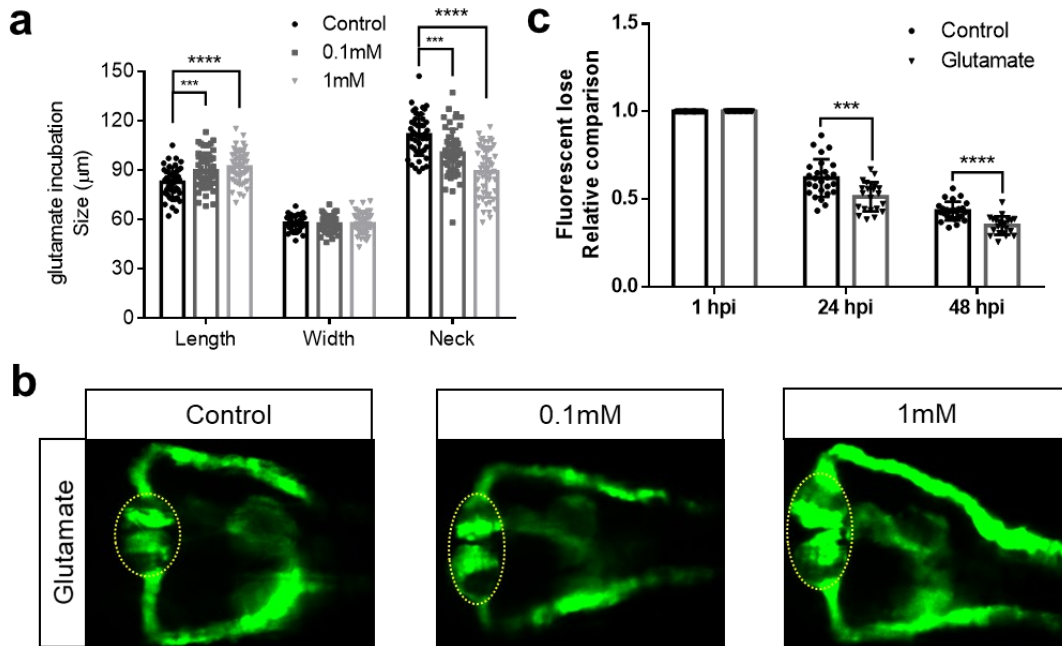


**Figure 15: Glutamate accumulation in *akr1a1b*<sup>-/-</sup> mutants damaged the kidneys**

(a, b) Enlarged glomerulus (encircled) and shortened tubular neck length in zebrafish embryos treated with glutamate (n = 46 in control group; n = 50 in 0.1mM group; n = 49 in 1mM group, mean  $\pm$  SD). (c) A significant increased loss of fluorescence in 1mM glutamate treated wild-type larvae (n = 26 in control group; n = 21 in 1mM group, mean  $\pm$  SD). \* p < 0.05, \*\*\* p < 0.001, \*\*\*\* p < 0.0001, p value of a, b, e was calculated by t-test, p value c was calculated by one-way ANOVA, Scale bar: 0.1 mm.



## Result

In zebrafish treated with 1 mM and 5 mM alanine, the glomerular length was increased to  $75.8 \pm 8.5 \mu\text{m}$  and  $87.1 \pm 6.1 \mu\text{m}$ , respectively, while it was  $77.6 \pm 11.3 \mu\text{m}$  in control conditions. The pronephric neck was shortened to  $127.2 \pm 15.6 \mu\text{m}$  and  $105.4 \pm 9.3 \mu\text{m}$ , respectively, while it was  $131.4 \pm 22.0 \mu\text{m}$  in egg water (Fig. 16a, b). In conclusion, although both amino acids induced pronephric alterations, glutamate (0.1 mM) was more detrimental than alanine (5 mM). These results suggest glutamate as the main damaging factor of pronephric changes in *akr1a1b*<sup>-/-</sup> zebrafish embryos.

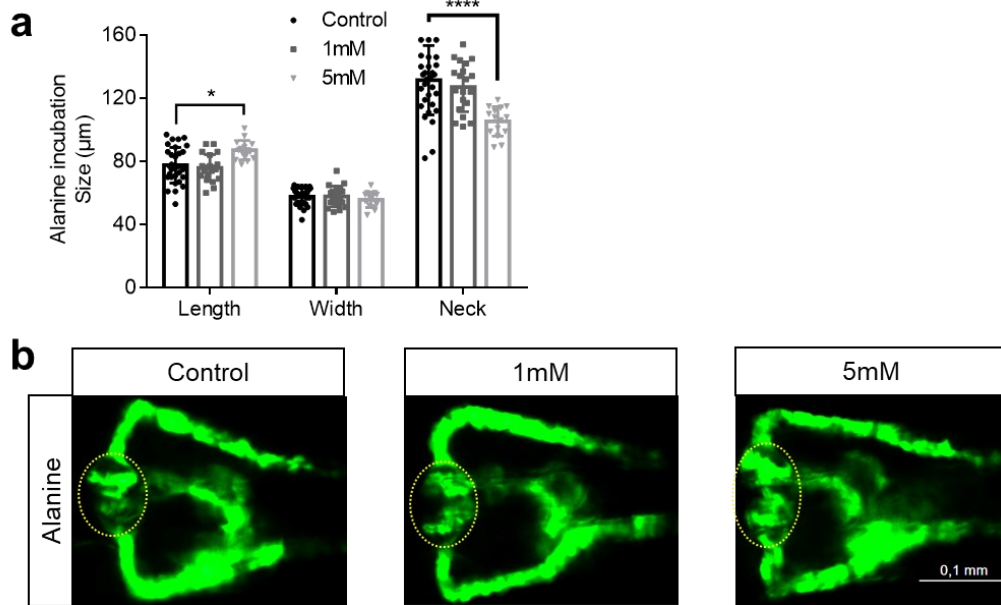


**Figure 16: Alanine accumulation in *akr1a1b*<sup>-/-</sup> mutants slightly damaged the kidneys**

(a, b) Enlarged glomerulus (encircled) and shortened tubular neck length in zebrafish embryos treated with alanine (n = 31 in control group; n= 20 in 0.1mM group; n= 15 in 1mM group , mean  $\pm$  SD). \*  $p < 0.05$  , \*\*\*  $p < 0.001$ , \*\*\*\*  $p < 0.0001$ . Scale bar: 0.1 mm.

Next, I aimed to verify whether the accumulation of glutamate and alanine persisted into adult zebrafish. Therefore, I measured concentrations of both amino acids in the kidneys and livers at 2 hours, 3 hours and 18 hours postprandial. Glutamate was significantly enriched in *akr1a1b*<sup>-/-</sup> adult zebrafish kidneys at 3 hours postprandial stage, to  $2.90 \pm 0.29 \text{ nmol/mg tissue}$ , and at 18 hours postprandial stage, to  $6.63 \pm 1.29 \text{ nmol/mg tissue}$ ; meanwhile, it was  $1.96 \pm 0.15 \text{ nmol/mg tissue}$  and  $3.14 \pm 0.37 \text{ nmol/mg tissue}$  in

## Result

*akr1a1b*<sup>+/+</sup> zebrafish kidneys, respectively (Fig. 17a). In contrast, the concentration of alanine was unchanged in kidneys as it was for glutamate and alanine in adult livers (Fig. 16b-d). Thus, increased concentrations of glutamate were only identified in *akr1a1b*<sup>-/-</sup> kidneys.

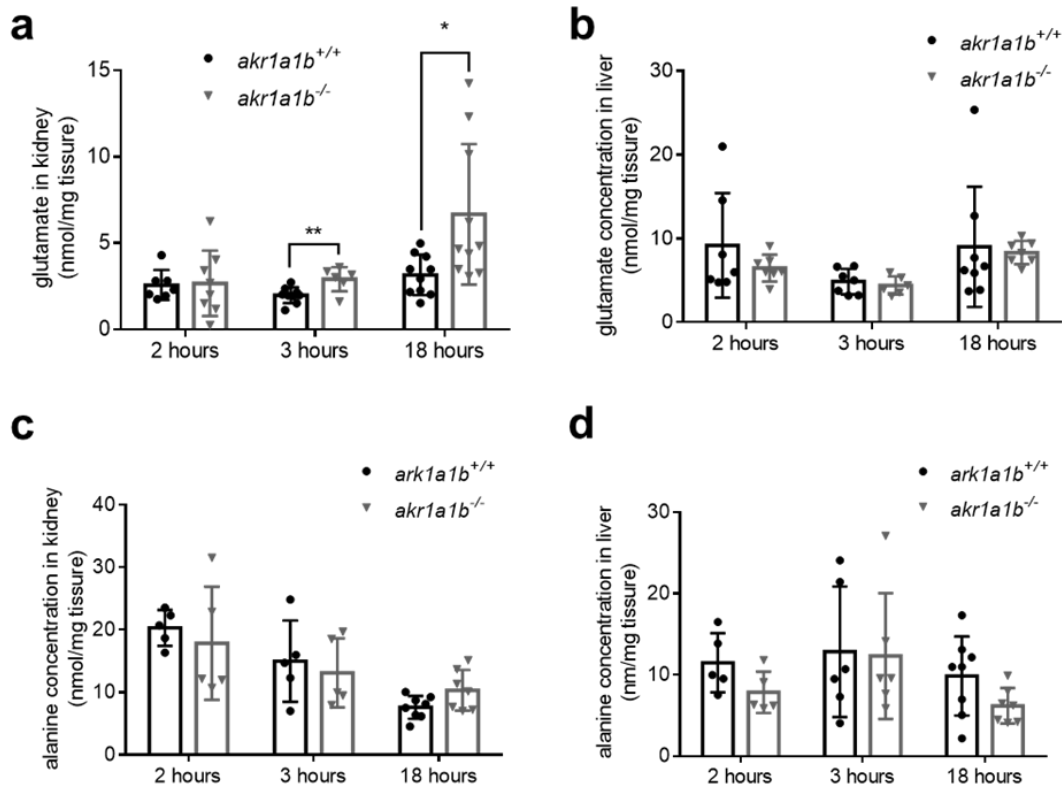


**Figure 17: Glutamate accumulation in *akr1a1b*<sup>-/-</sup> zebrafish kidneys**

(a) Glutamate accumulated in adult *akr1a1b*<sup>-/-</sup> zebrafish kidneys at 3 hours and 18 hours postprandial (2 hours postprandial: n= 7 in *akr1a1b*<sup>+/+</sup>, n= 8 in *akr1a1b*<sup>-/-</sup>; 3 hours postprandial: n= 9 in *akr1a1b*<sup>+/+</sup>, n= 6 in *akr1a1b*<sup>-/-</sup>; 18 hours postprandial: n= 10 in both groups, mean  $\pm$  SD). (b) Unaltered concentrations of glutamate in adult *akr1a1b*<sup>-/-</sup> livers (2 hours postprandial: n= 7 in *akr1a1b*<sup>+/+</sup>, n= 7 in *akr1a1b*<sup>-/-</sup>; 3 hours postprandial: n= 7 in *akr1a1b*<sup>+/+</sup>, n= 6 in *akr1a1b*<sup>-/-</sup>; 18 hours postprandial: n= 8 in *akr1a1b*<sup>+/+</sup>, n= 7 in *akr1a1b*<sup>-/-</sup>, mean  $\pm$  SD). (d, e) Concentrations of alanine were not altered in adult *akr1a1b*<sup>-/-</sup> kidneys (2 hours postprandial: n= 5 in *akr1a1b*<sup>+/+</sup>, n= 5 in *akr1a1b*<sup>-/-</sup>; 3 hours postprandial: n= 5 in *akr1a1b*<sup>+/+</sup>, n= 5 in *akr1a1b*<sup>-/-</sup>; 18 hours postprandial: n= 8 in *akr1a1b*<sup>+/+</sup>, n= 7 in *akr1a1b*<sup>-/-</sup>, mean  $\pm$  SD) and in adult *akr1a1b*<sup>-/-</sup> livers (2 hours postprandial: n= 5 in *akr1a1b*<sup>+/+</sup>, n= 5 in *akr1a1b*<sup>-/-</sup>; 3 hours postprandial: n= 5 in *akr1a1b*<sup>+/+</sup>, n= 6 in *akr1a1b*<sup>-/-</sup>; 18 hours postprandial: n= 8 in *akr1a1b*<sup>+/+</sup>, n= 7 in *akr1a1b*<sup>-/-</sup>, mean  $\pm$  SD).

### 3.5 Altered gluconeogenesis in *akr1a1b*<sup>-/-</sup> zebrafish

Glutamate and alanine are glucogenic amino acids serving as primary substrates for gluconeogenesis in kidneys and livers, respectively. The accumulation of glutamate in *akr1a1b*<sup>-/-</sup> embryos and in adult *akr1a1b*<sup>-/-</sup> kidneys led to the hypothesis of dysfunctional gluconeogenesis, specifically in kidneys. Glucose synthesis by gluconeogenesis in the kidney accounts for approximately 20% of total glucose production in the body in the post-absorptive state<sup>(Gerich et al., 2001)</sup>, and alterations of glucose synthesis may affect glucose homeostasis. In order to test if glucose homeostasis is altered in adult *akr1a1b*<sup>-/-</sup> mutants, I measured blood glucose concentrations of adult zebrafish at 2 hours, 3 hours and 18 hours postprandial. I found hypoglycemia after overnight fasting with blood glucose concentrations of  $26.12 \pm 5.50$  mg/dl in *akr1a1b*<sup>-/-</sup> zebrafish significantly lower compared with  $34.29 \pm 15.66$  mg/dl in *akr1a1b*<sup>+/+</sup> zebrafish (Fig. 18). Yet, blood glucose levels two and three hours after feeding were not changed in *akr1a1b*<sup>-/-</sup> zebrafish, indicating physiological glucose metabolism after glucose uptake. Thus, the data suggest inhibition of gluconeogenesis in *akr1a1b*<sup>-/-</sup> mutants, especially in kidneys, since renal gluconeogenesis accounts for the major glucose production in the prolonged fasting stage.

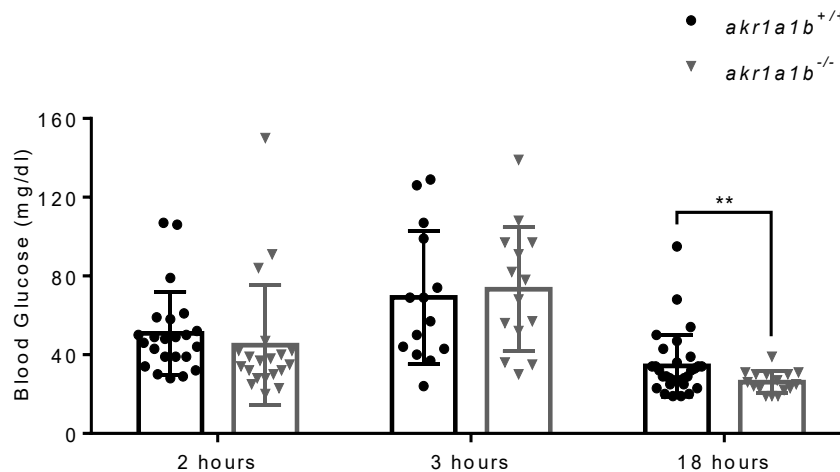


**Figure 18: hypoglycemia was found in overnight fasted *akr1a1b*<sup>-/-</sup> zebrafish**

Blood glucose was measured at different time points after feeding in adult *akr1a1b*<sup>+/+</sup> and *akr1a1b*<sup>-/-</sup> zebrafish, and found hypoglycemia after overnight fasting in *akr1a1b*<sup>-/-</sup> zebrafish (2 hours postprandial: n= 23 in *akr1a1b*<sup>+/+</sup>, n= 20 in *akr1a1b*<sup>-/-</sup>; 3 hours postprandial: n= 14 in *akr1a1b*<sup>+/+</sup>, n= 14 in *akr1a1b*<sup>-/-</sup>; 18 hours postprandial: n= 31 in *akr1a1b*<sup>+/+</sup>, n= 16 in *akr1a1b*<sup>-/-</sup>, mean  $\pm$  SD).

## Result

Gluconeogenesis is regulated by different mechanisms. Amongst the genes involved in gluconeogenesis regulation, the critical rate-limiting enzyme is PEPCK, whose activity is directly related by its mRNA abundance<sup>(Quinn and Yeagley, 2005)</sup>. Thus, I compared PEPCK expression in livers and kidneys between *akr1a1b*<sup>+/+</sup> and *akr1a1b*<sup>-/-</sup> adult zebrafish after 2 hours, 3 hours, and 18 hours postprandial. It was found that PEPCK expression 2 hours after feeding remained unaltered in *akr1a1b*<sup>-/-</sup> livers and kidneys, while 3 hours and 18 hours postprandial, PEPCK expression in *akr1a1b*<sup>-/-</sup> kidneys was significantly reduced (Fig. 19a, b). Together, the data indicated that *akr1a1b* deficiency in zebrafish blocks PEPCK expression in kidneys leading to inhibition of gluconeogenesis, accompanied by long-lasting hypoglycemic episodes and renal glutamate accumulation promoting kidney alterations.

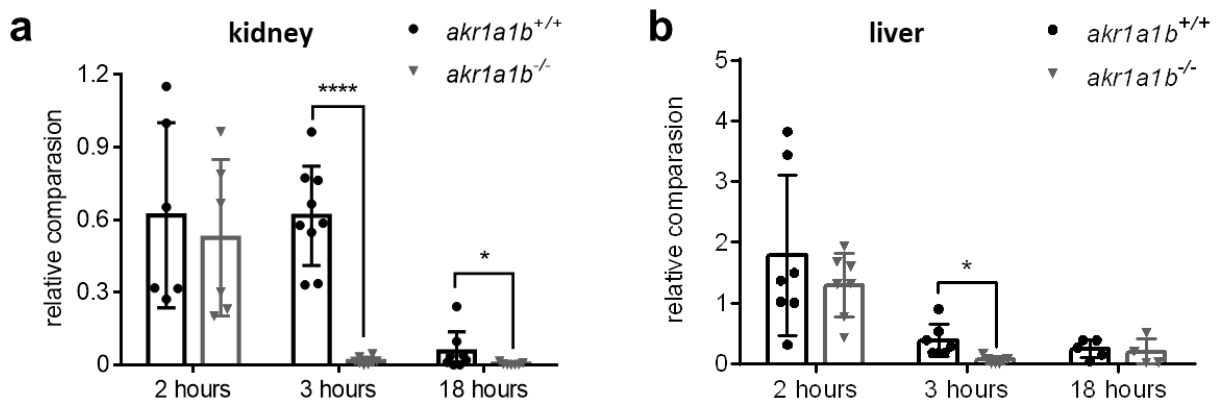


**Figure 19: Inhibition of gluconeogenesis led to the hypoglycemia in overnight fasted *akr1a1b*<sup>-/-</sup> zebrafish**

(a) Loss of cytosolic PEPCK expression in adult *akr1a1b*<sup>-/-</sup> kidneys 3 hours and 18 hours after feeding (2 hours postprandial: n= 6 in *akr1a1b*<sup>+/+</sup>, n= 6 in *akr1a1b*<sup>-/-</sup>; 3 hours postprandial: n= 9 in *akr1a1b*<sup>+/+</sup>, n= 8 in *akr1a1b*<sup>-/-</sup>; 18 hours postprandial: n= 8 in *akr1a1b*<sup>+/+</sup>, n= 7 in *akr1a1b*<sup>-/-</sup>, mean ± SD). (b) Loss of cytosolic cPEPCK expression in *akr1a1b*<sup>-/-</sup> livers 3 hours after feeding (2 hours postprandial: n= 7 in *akr1a1b*<sup>+/+</sup>, n= 7 in *akr1a1b*<sup>-/-</sup>; 3 hours postprandial: n= 7 in *akr1a1b*<sup>+/+</sup>, n= 7 in *akr1a1b*<sup>-/-</sup>; 18 hours postprandial: n= 5 in *akr1a1b*<sup>+/+</sup>, n= 4 in *akr1a1b*<sup>-/-</sup>, mean ± SD). cPEPCK expression was analyzed by RT-qPCR and normalized to *b2m*. \*p<0.05, \*\*p<0.01, \*\*\*\*p<0.0001.

### 3.6 Akr1a1b regulates S-nitrosylation

A recent study in mice has proven that Akr1a1 mediates glucose metabolism by inhibiting S-nitrosylation of glycolytic enzymes. Thus, we hypothesized an altered S-nitrosylation as the upstream mechanism regulating kidney malformation in *akr1a1b*<sup>-/-</sup> mutants. First, we determined nitrotyrosine as marker for nitrosative stress in 96hpf *akr1a1b*<sup>-/-</sup> larvae and found a significant increase (Fig. 20a). Secondly, SNOs (S-nitrosylated proteins) levels were measured by Western blot, and it was found that SNOs were highly increased in livers of *akr1a1b*<sup>-/-</sup> zebrafish (Fig. 20b). These data pointed to an increased stimulation of S-nitrosylation in *akr1a1b*<sup>-/-</sup> zebrafish.

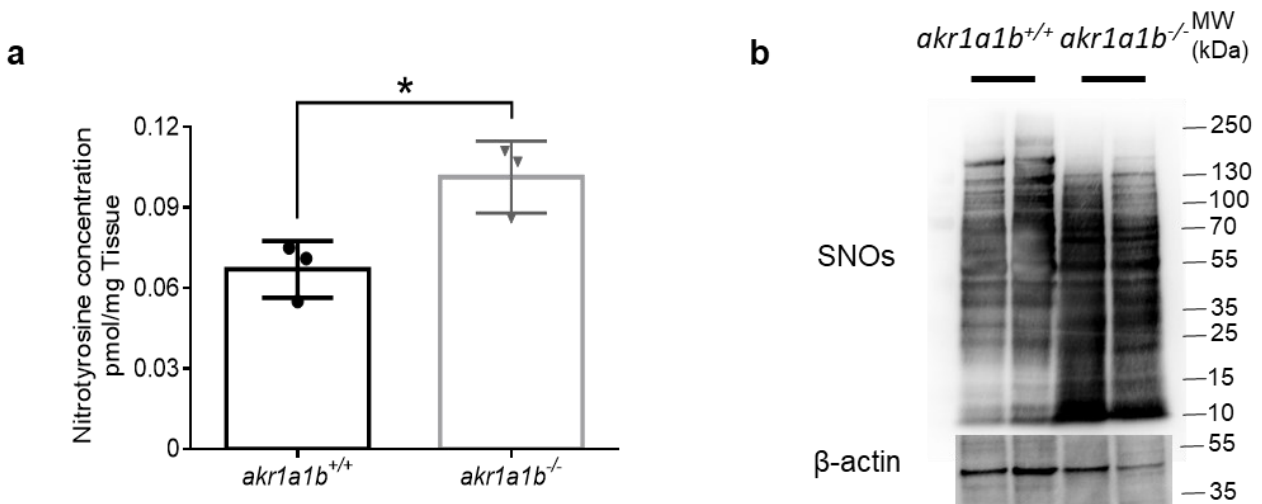


**Figure 20: Accumulation of S-nitrosylated proteins in *akr1a1b*<sup>-/-</sup> mutants**

(a) Nitrotyrosine was measured by UPLC-MS, and was increased in 96 hpf *akr1a1b*<sup>-/-</sup> larvae (n = 3 clutches with 50 larvae, mean ± SD). (b) Western blots show increased S-nitrosylated proteins (SNOs) in *akr1a1b*<sup>-/-</sup> livers (n = 2).

## Result

To investigate whether evaluated S-nitrosylation may account for kidney alterations observed in *akr1a1b*<sup>-/-</sup> embryos. *Akr1a1b*<sup>+/+</sup> and *akr1a1b*<sup>-/-</sup> embryos were treated with 20  $\mu$ M L-NAME, a known inhibitor of nitric oxide formation. It was found that inhibition of S-nitrosylation by L-NAME treatment in *akr1a1b*<sup>-/-</sup> embryos normalized the alterations of the pronephros at 48 hpf (Fig. 21a, b).

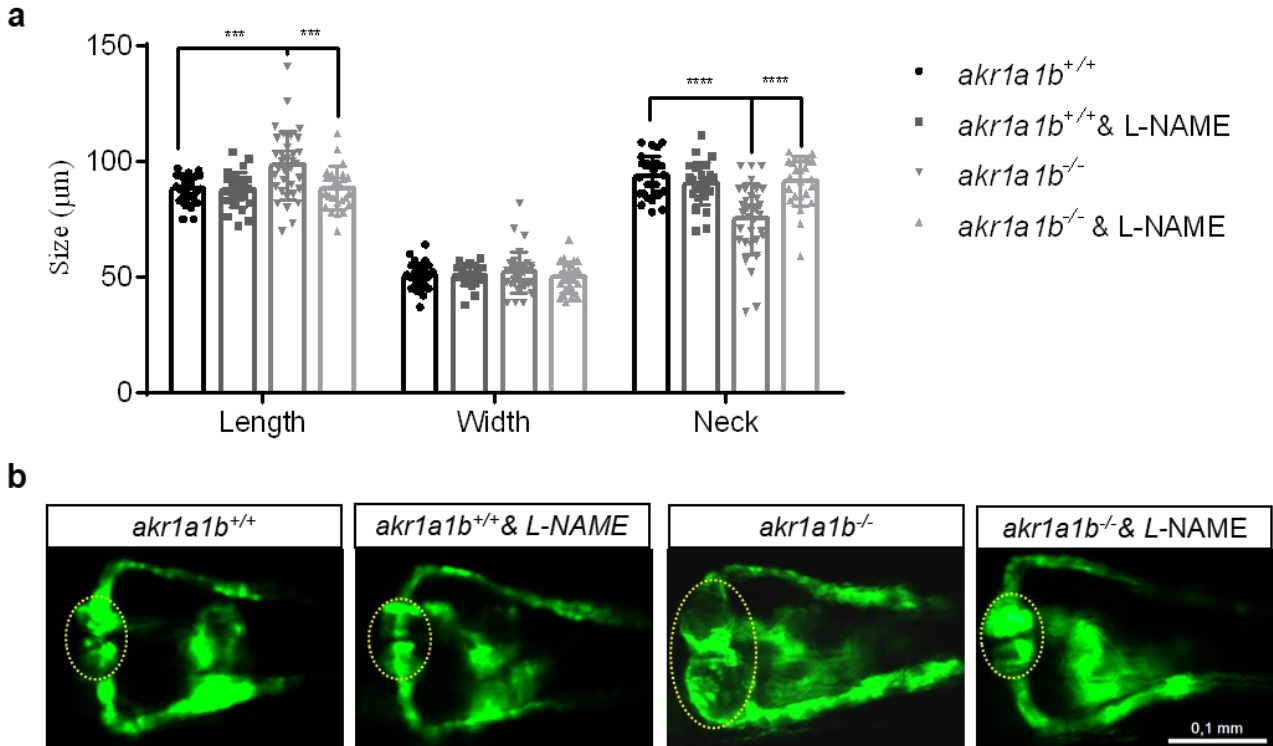


**Figure 21: NO-dependent S-nitrosylation regulated gluconeogenesis and pronephros development in *akr1a1b*<sup>-/-</sup> mutants**

(a, b) Inhibition of NO-dependent S-nitrosylation by L-NAME in *akr1a1b*<sup>-/-</sup> zebrafish embryos rescued the altered pronephros (n = 27 in *akr1a1b*<sup>+/+</sup> group; n = 27 in *akr1a1b*<sup>+/+</sup> & L-NAME group; n = 34 in *akr1a1b*<sup>-/-</sup> group; n = 25 in *akr1a1b*<sup>-/-</sup> & L-NAME group, mean  $\pm$  SD)., \*\*\*p<0.001, \*\*\*\*p<0.0001. Scale bar: 0.1 mm.

## Result

In addition, I analyzed if PEPCK expression is regulated by S-nitrosylation and therefore determined PEPCK expression in 96 hpf *akr1a1b*<sup>-/-</sup> larvae after L-NAME treatment. It was found that PEPCK expression is increased in 96 hpf L-NAME treated *akr1a1b*<sup>+/+</sup> larvae, while PEPCK expression in *akr1a1b*<sup>-/-</sup> larvae compared to *akr1a1b*<sup>+/+</sup> larvae was slightly decreased, but could be significantly increased and normalized to *akr1a1b*<sup>+/+</sup> levels after the L-NAME treatment (Fig. 22). Altogether, the data have proven that altered gluconeogenesis and glutamate accumulation in *akr1a1b*<sup>-/-</sup> zebrafish caused by enriched SNOs accounted for the underlying kidney abnormalities.

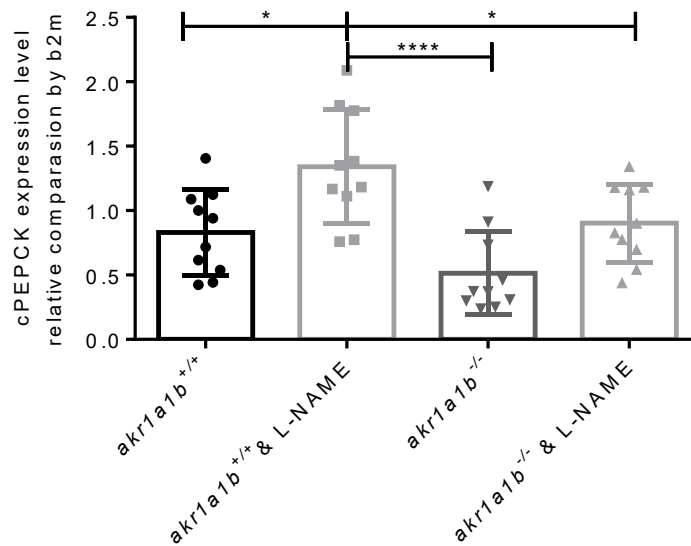


**Figure 22: NO-dependent S-nitrosylation regulated gluconeogenesis in zebrafish larvae at 96 hpf**

cPEPCK expression was regulated by S-nitrosylation. Inhibition of S-nitrosylation by L-NAME treatment increased cPEPCK expression in *akr1a1b*<sup>+/+</sup> and *akr1a1b*<sup>-/-</sup> embryos at 96 hpf and normalized cPEPCK expression in *akr1a1b*<sup>-/-</sup> embryos as measured by RT-qPCR (n = 10 in all groups, mean ± SD). \*p<0.05, \*\*\*\*p<0.0001.

## 4 DISCUSSION

In this study, we have established for the first time of an *akr1a1b* knockout animal model in zebrafish, and the main findings are summarized in Fig. 23. My data show that: 1) Akr1a1 protein shares high similar amino acid sequence among zebrafish, human and mouse with a highly conserved active site. 2) Akr1a1b was abundantly expressed throughout embryonic and larval stages and also in all analyzed adult organs with being highest expressed in livers. 3) *Akr1a1b* knockout in zebrafish caused alterations of the embryonic pronephros and of adult kidneys. 4) Loss of *akr1a1b* leads to hypoglycemia and glutamate accumulation, which severely damages the pronephros, and NO-dependent S-nitrosylation regulates this process. 5) Akr1a1b regulates the S-nitrosylation process.

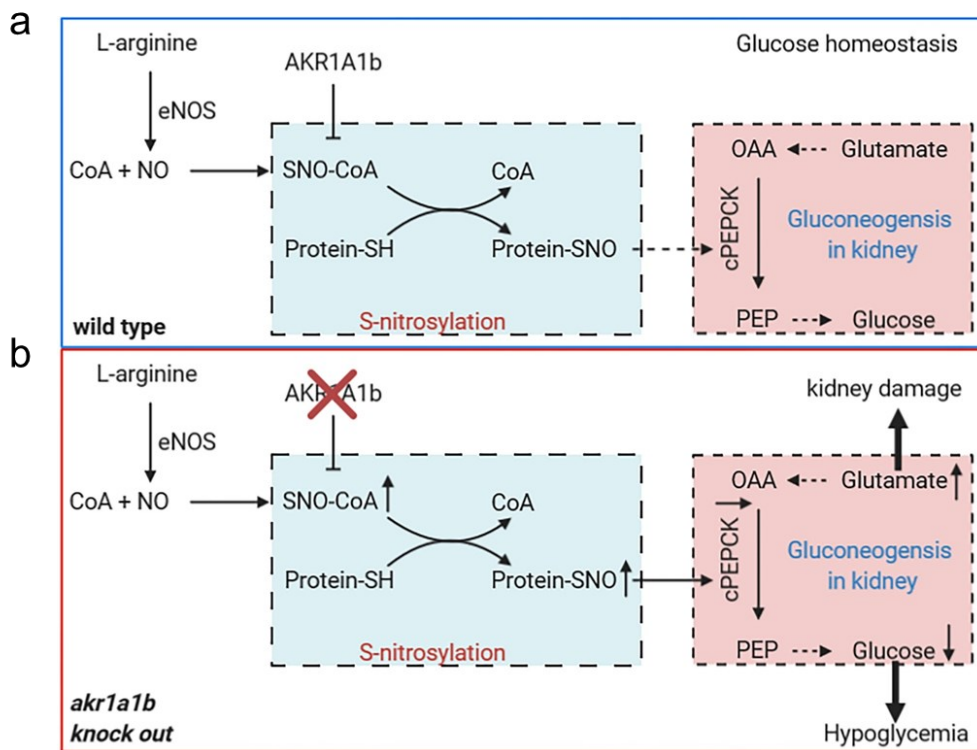


**Figure 23: Akr1a1b regulates NO-dependent gluconeogenesis**

**(a)** Akr1a1b balances NO-dependent S-nitrosylation of proteins and thereby regulates expression of PEPCK. In fasting state, kidneys use glutamate as substrate for gluconeogenesis, generate glucose and thus regulating glucose homeostasis. **(b)** In absence of Akr1a1b, S-nitrosylation is increased and blocks PEPCK expression. Subsequently, glutamate accumulates and zebrafish develop fasting hypoglycemia.



### 4.1 *Akr1a1b* expression in zebrafish

Although Aldo-keto reductase superfamily exists in virtually all organisms, database research on three different platforms (NCBI <sup>1</sup>, Ensembl <sup>2</sup>, Aldo-Keto Reductase Superfamily homepage<sup>3</sup>) showed *Akr1a1* genes expression only in animals. Although *akr1a1* names are differently: *akr1a2* in the pig<sup>(Ye et al., 2001)</sup>, *akr1a3* in the rat<sup>(MacLeod et al., 2010)</sup>, and *akr1a4* in the mouse<sup>(Allan and Lohnes, 2000)</sup>, all these homolog enzymes structurally and functionally similar<sup>(Allan and Lohnes, 2000; Bohren et al., 1989; Flynn et al., 1995; Takahashi et al., 1993; Wermuth et al., 1987)</sup>.

Unlike other animals, two separate *akr1a1* genes exist in zebrafish, namely *akr1a1a* and *akr1a1b*, whose functions have not been studied yet. Therefore, I investigated the protein sequence first. The alignment data showed that *Akr1a1b* in zebrafish and *Akr1a1* in the human and mouse displayed similar signal peptide sequences, and one conserved enzyme active site (tyrosine) among these three different species. Thus, zebrafish *Akr1a1b* might function physiologically like mammalian *Akr1a1*, while is also implied that *akr1a1b* knockout zebrafish is a novel and appropriate model for studying human *Akr1a1* in physiological and pathological functional studies.

The qPCR investigation showed that *akr1a1b* is expressed in very early developmental stages, in the first day after birth, which indicated an essential function of this enzyme for the physiological development of zebrafish embryos. Besides, considering the oxidoreductive functions of the *Akr* enzymes, the data also indicates that reactive oxygen species (ROS) appear in embryos early and need to be adequately detoxified ensuring embryonic survival. Interestingly, some studies proved that although ROS's moderate level is beneficial<sup>(Forman et al., 2010; Handy and Loscalzo, 2012)</sup>, a higher concentration of ROS leads to decreased and even arrested embryonic development<sup>(Favetta et al., 2007; Zhang et al., 2010)</sup>. Consistent with this theory, we found an increased methylglyoxal concentration, measured by LC-MS/MS, in *akr1a1b* deficiency zebrafish larvae at 96 hpf. However, different from *Akr1a1*, which is highly expressed in the kidney in humans and

---

<sup>1</sup> <https://www.ncbi.nlm.nih.gov/gene/?term=akr1a1>, accessed on the 12.06.2020.

<sup>2</sup> <https://www.ensembl.org/Multi/Search/Results?q=akr1a1>, accessed on the 12.06.2020.

<sup>3</sup> <https://hosting.med.upenn.edu/akr/family-tree-structures/>, accessed on the 12.06.2020.

rodents<sup>(Fagerberg et al., 2014; Yu et al., 2014; Yue et al., 2014)</sup>, *Akr1a1b* presents the highest expression level in the liver of adult zebrafish. Recent studies showed high *akr1a1* expression in proximal renal tubules<sup>(MacLeod et al., 2010; Zhou et al., 2019)</sup>, which is consistent with zebrafish verified by immunohistochemistry technology. All these data suggested that *akr1a1b* is a homolog of *akr1a1* in mammals with similar functions.

### 4.2 *Akr1a1b* deficiency affects zebrafish renal development and functionality by accumulating glutamate

Previous studies suggested *Akr* enzymes involved in several kidney diseases. Upregulated *Akr1b1* promotes a higher level of polyol pathway flux under the hyperglycemic condition, further causing diabetic nephropathy<sup>(Alexiou et al., 2009)</sup>. It has recently been reported that *Akr* genes were compensatory upregulated in the *Glo1*<sup>-/-</sup> mice to maintain MG at normal level keeping livers and kidneys healthy<sup>(Schumacher et al., 2018)</sup>. Increased *Akr* proteins in transplanted kidneys might be a reason to attenuate the course of delayed graft function<sup>(Wijermars et al., 2018)</sup>. Knock-out of *akr1a1* in acute kidney injury mice protected against the disease and improved survival<sup>(Zhou et al., 2019)</sup>. Yet, the physiological role of *Akr1a1* under non-disease conditions is still unknown.

Although many *in vivo* / *vitro* studies have revealed the physiological and pathological role of *Akr1a1* of mammals, there is no research about *akr1a1b* function up to date. Therefore, in this study we established the *akr1a1b* knock-out zebrafish model by using CRISPR-Cas9 technology and evaluated the function of this enzyme for the first time. By enzyme activity determination and western blot, we validated successfully the knockout of *akr1a1b* by showing the loss of *Akr1a1b* activity and protein expression in both mutants. However, the activity assay didn't show a 100% loss of *Akr* activity. This can most likely be explained by the broad substrate utilization among all *Akr* enzymes in zebrafish and the activity assay, we performed could not be specifically targeted to only *Akr1a1b*, but also includes *Akr1a1a* and *Akr1b1* activities.

Based on the pronephric alteration, we hypothesized that the knockout of *akr1a1b* may cause a non-temporary developmental phenotype. Therefore, histological staining and electron microscopy on adult zebrafish kidney tissues were conducted and confirmed this hypothesis. By using a metabolic screening approach for *akr1a1b*<sup>-/-</sup> zebrafish larvae, I found significant alterations of some intermediates of glucose metabolism, including

citrate, glutamate, 2-keto-glutarate, and alanine. Interestingly, various studies have shown the toxic effects of glutamate on animals' kidney. Due to the presence of glutamate receptors identified in kidneys<sup>(Du et al., 2016)</sup>, high monosodium glutamate (MSG) diet might induce hypothalamic toxicity, higher oxidative stress, hyperinsulinemia, low hepatic glycogen concentration in the liver, and impaired oral glucose tolerance test and hyperglycemia in fasted and postprandial rat<sup>(Diniz et al., 2004)</sup>. Also, injected MSG altered free radical enzymes in cardiac tissue, thereby induced oxidative stress<sup>(K. Sing, 2005)</sup>. Chronic consumption of dietary MSG causes obstructive nephropathy from urolithiasis in adult rats with significantly increased renal interstitial fibrosis<sup>(Sharma et al., 2013)</sup>. Intraperitoneally administered MSG in rat caused variable pathological alterations of the glomerular, including hypercellularity and thickening capillary membrane. It also showed a significant difference in glomeruli with an increase in the bowman's capsule's length and size, and bowman's space.<sup>(Dixit et al., 2014)</sup>. On the other hand, elevated blood or plasma glutamate levels have been shown in patients with chronic renal failure<sup>(Raj et al., 2005)</sup>. Taken together, these suggested that an excess of glutamate seems to be toxic to the kidney.

Therefore, it appears that excessive glutamate in *akr1a1b* knockout embryos might be the reason for the alteration of the pronephros. This hypothesis has been validated by glutamate treatment of embryos/ larvae in our study. The data showed that treated with glutamate, embryonic pronephros and larvae kidney function were altered, which is similar to the observed changes in *akr1a1b* mutants. Interestingly, I found the increase of glutamate level persisted into adult in *ark1a1b* deficient zebrafish kidneys accompanied with a slight, but significant thicker glomerular membrane, and much more droplets in proximal tubules. This is a further illustration of the toxic effect of elevated glutamate in kidneys. It has been reported that the glomerular basement membrane, a kind of specialized extracellular matrix, is partially developed from podocytes during the glomerulogenesis<sup>(Abrahamson, 2012)</sup>. Besides, more and more studies support the observations that several glutamate receptors are present in a serious of glomerular cells, including podocyte<sup>(Dryer, 2015; Gu et al., 2012; Wang et al., 2019)</sup>, and dysregulation of glutamate signaling can induce albuminuria and glomerular damage in mice<sup>(Puliti et al., 2011)</sup>. Therefore, the thicker glomerular membrane in *akr1a1b* knockout kidneys might also

result from the glutamate elevation. Nevertheless, the mechanism of the pathological role of glutamate to kidney lesion is still needed further study.

### 4.3 Inhibitory of gluconeogenesis leads to the glutamate accumulation

In this study, I showed hypoglycemia in *akr1a1b* knockout adult zebrafish at fasting, but not during the postprandial stage. The data indicated dysfunctional gluconeogenesis. Gluconeogenesis is a glucose-producing process, which is very important in keeping physiological blood glucose levels in fasted animals. Organs, especially the brain, need an appropriate continuous supply of glucose throughout the whole day. Therefore, different pathways are needed to regulate blood glucose during postprandial, post-absorptive /fasting, and starvation state.

After a meal, the first stage is the postprandial or absorptive stage that lasts for around 4 hours. Increased plasma glucose, uptaken from food, promotes the release of insulin, which triggers glycolysis and glycogenesis, subsequently lowers blood glucose to normal level. During the post-absorptive/ fasting state, glucagon starts releasing and is raising blood glucose. Liver cells begin using their glycogen stores to convert into glucose in response to the glucagon's rising level. After about four hours of liver glycogenolysis, liver stores become depleted, and blood glucose concentration fall. Therefore, gluconeogenesis plays a more critical role in the late fasting and the following starvation stage for generating glucose and maintaining the blood glucose level.

Gluconeogenesis mainly uses three main precursors: lactate, glycerol, and amino acids, estimating for more than 90% of overall producing-glucose<sup>(Gerich, 1993)</sup>. Lactate is the most important substrate for gluconeogenesis both in the liver and kidney<sup>(Conjard et al., 2001)</sup>, and it is responsible for around 60% of renal gluconeogenesis<sup>(Alsahli and Gerich, 2017)</sup>. However, during prolonged fasting state, muscle-derived amino acids are the most important substrates for the production of glucose in a prolonged fasting status<sup>(Ruderman, 1975)</sup>. The reason for the lactate-glucose pathway switch to gluconeogenic amino acids-glucose pathway might be, the lactate is produced by glycolysis, from glucose itself, but amino acids are digested from muscle protein.

Interestingly, a couple of studies have identified a substrate preference for gluconeogenesis in different organs: the kidney prefers glutamate, whereas the liver

preferentially uses alanine<sup>(Stumvoll et al., 1999)</sup>. Besides, some studies showed that renal cortical glutamate levels and renal gluconeogenesis are related. The increased gluconeogenesis via glutamate pathway caused the fall of cortical glutamate concentration; conversely, when decreased cortical gluconeogenic capacity was observed, renal glutamate content is boosted in rats<sup>(Pagliara and Goodman, 1970)</sup>. Thus, I proposed that the increased glutamate concentration in *akr1a1b* deficient zebrafish larvae and adult kidneys resulted from the inhibition of renal gluconeogenesis, which revealed by sharp downregulation of cPEPCK expression of kidney measured by qPCR technology. Therefore, the question became that why gluconeogenesis was inhibited in *akr1a1b* mutants.

#### 4.4 Ak1a1b regulates S-nitrosylation

Nitric oxide (NO) is a short-lived, gaseous, free radical gasotransmitter generated in various types of cells, including but not limited to endothelial, neuronal, muscle, and immune cells, by using L-arginine as the substrate. The process is catalyzed by three isoforms of the NO synthase (NOS): neuronal NOS (nNOS/ NOS1), inducible NOS (iNOS/ NOS2) and endothelial NOS (eNOS/ NOS3)<sup>(Bredt and Snyder, 1990)</sup>. However, free-NO only exists inside cells for 3-4 seconds<sup>(Feelisch, 1993)</sup>. It is rapidly utilized by proteins nearby, then most NO ions are stored as nitrosyl adducts on to Cys-thiol of proteins via the S-nitrosylation (SNO) pathway<sup>(Hess et al., 2005)</sup>. In fact, similar to the phosphorylation process, the SNO pathway was also identified as a post-translational modification of proteins. It plays an important role, the same as the phosphorylation pathway<sup>(Nakamura and Lipton, 2013)</sup>. Moreover, because of the structural alteration effects of protein triggered by S-nitrosylation, it can regulate other post-translational modifications, such as phosphorylation<sup>(Murillo-Carretero et al., 2009)</sup>, acetylation<sup>(Kornberg et al., 2010)</sup>, S-Palmitoylation<sup>(Hess et al., 1993)</sup>, ubiquitination<sup>(Li et al., 2007)</sup>, and Cys-based redox modifications<sup>(West et al., 2006)</sup>. To date, more than 3000 proteins are reported to be affected by S-nitrosylation<sup>(Hess and Stamler, 2012)</sup>, and are involved in a series of physiological processes, including protein stability, transcription control, DNA damage restoration, cellular growth/ differentiation/ apoptosis, and redox regulation<sup>(Fernando et al., 2019)</sup>.

Interestingly, the activity of proteins altered differently after S-nitrosylation. Under physiological conditions, normal levels of SNO keep many proteins inactive; meanwhile,

it lets many other proteins obtain full active. For example, three enzymes, Hexokinase/Glucokinase (HK/GK), Phosphofructokinase (PFK) and pyruvate kinase (PK), are the rate-limiting factors in the glycolysis process. It has been shown that SNO upregulates the activity of GK<sup>(Rizzo and Piston, 2003)</sup>, but blocked the PK activity<sup>(Zhou et al., 2019)</sup>. Furthermore, it has also been reported that SNO indirectly upregulates PFK activity via the AMPK pathway activation<sup>(Almeida et al., 2004)</sup>.

Surprisingly, a recent study identified the Akr1a1 enzyme as a novel SNO-CoA reductase (SCoR), which de-nitrosylates SNO-proteins in a CoA-dependent manner. The deletion of Akr1a1 protein in mice led to an increased S-nitrosylation of pyruvate kinase M2 (PKM2), thereby down-regulated its activity<sup>(Zhou et al., 2019)</sup>. Consistently, we found the same SNO regulation in *akr1a1b* knock-out zebrafish in our study, which was proved by the western blot technology. Firstly, it implied Akr1a1b's function as a SCoR in zebrafish should be the same as Akr1a1 in the mouse, which suggests that *akr1a1b*<sup>-/-</sup> zebrafish is a good model for investigating the physiological and pathological function of human *akr1a1* gene. Secondly, the increased whole amount of SNO-proteins (SNOs) can explain why gluconeogenesis was inhibited.

One hypothesis is that increased PFK activity caused by SNO activates glycolysis, thereby inhibiting glycolysis's reversal processes - gluconeogenesis. The other hypothesis is that SNO can decrease the cPEPCK level directly. In our study, we proved the second hypothesis. L-NAME is a NOS inhibitor that can block the process of SNO. After treatment with L-NAME, the pronephric alterations in *akr1a1b*<sup>-/-</sup> zebrafish embryos could be rescued. Moreover, the cPEPCK gene was significantly up-regulated in *akr1a1b*<sup>+/+</sup> zebrafish larvae treated by L-NAME, and in addition, the effect was normalized in *akr1a1b*<sup>-/-</sup> larvae. These data indicated that the increased SNO caused by *akr1a1b* knockout in zebrafish resulted in the pronephric alteration on the one hand. On the other hand, the up-regulated cPEPCK expression caused by L-NAME was normalized by the deletion of Akr1a1b. Altogether, it appears that cPEPCK gene expression is linked to the cellular SNO levels.

In agreement with the above data, some studies showed the same phenomenon. Chronic nicotine treatment on insulin-sensitive C57BL/J6 mice caused an increased buildup of NO in plasma and liver, along with simultaneous suppression of cPEPCK and

G6Pase mRNA level<sup>(Vu et al., 2014)</sup>. Both long and short term treatment of rats with leptin would have induced more NO production, accompanied by less expression of cPEPCK<sup>(Jaubert et al., 2012; Niang et al., 2011)</sup>. However, the mechanisms are still mostly unknown and needs further study.

## 5 SUMMARY

In this thesis, I analyzed the function of Akr1a1b in the zebrafish kidney. A series of experiments characterizing the kidney, glucose homeostasis, and metabolism after the loss of Akr1a1b were performed. The main findings of this dissertation are:

(1) *Akr1a1b*<sup>-/-</sup> zebrafish exhibit altered morphology and function of the pronephros. The metabolome data showed accumulated glutamate in *akr1a1b*<sup>-/-</sup> larvae and adult zebrafish kidneys. The altered pronephros in *akr1a1b*<sup>-/-</sup> larvae can be mimicked by glutamate treatment in *akr1a1b*<sup>+/+</sup> larvae, which indicated that *akr1a1b* deficiency led to zebrafish renal alteration by accumulated glutamate. Nevertheless, the mechanisms how glutamate leads to kidney lesions still needs further investigations.

(2) Hypoglycemia was found in overnight fasted *akr1a1b*<sup>-/-</sup> adult zebrafish and cPEPCK expression was inhibited in the kidney. cPEPCK catalyzes an irreversible step of gluconeogenesis through the glutamate-glucose pathway. Therefore, glutamate accumulates in the kidney under the condition of cPEPCK inhibition.

(3) The nitrotyrosine concentration and SNOs levels in *akr1a1b*<sup>-/-</sup> larvae and in adult *akr1a1b*<sup>-/-</sup> zebrafish livers were increased. These data pointed to an increased S-nitrosylation activity in *akr1a1b*<sup>-/-</sup> zebrafish. Importantly, phenotypes caused by *akr1a1b* deficiency in embryos/ larvae were normalized by L-NAME, which inhibits NOS and therefore, block S-nitrosylation. Altogether, the data have proven that altered kidney morphology, glutamate concentration, glucose homeostasis, and cPEPCK expression in *akr1a1b*<sup>-/-</sup> zebrafish are caused by increased S-nitrosylation. Thus, Akr1a1b regulates S-nitrosylation in zebrafish in the same way as Akr1a1 in mice.

In summary, I identified Akr1a1b as a novel regulator of gluconeogenesis in zebrafish via NO-dependent S-nitrosylation, thereby describing a novel regulator of glucose homeostasis.



## 6 REFERENCE

Abrahamson, D.R. (2012). Role of the podocyte (and glomerular endothelium) in building the GBM. *Semin Nephrol* 32, 342-349.

Alexiou, P., Pegklidou, K., Chatzopoulou, M., Nicolaou, I., and Demopoulos, V.J. (2009). Aldose reductase enzyme and its implication to major health problems of the 21(st) century. *Curr Med Chem* 16, 734-752.

Allan, D., and Lohnes, D. (2000). Cloning and developmental expression of mouse aldehyde reductase (AKR1A4). *Mech Dev* 94, 271-275.

Almeida, A., Moncada, S., and Bolanos, J.P. (2004). Nitric oxide switches on glycolysis through the AMP protein kinase and 6-phosphofructo-2-kinase pathway. *Nat Cell Biol* 6, 45-U49.

Alsahli, M., and Gerich, J.E. (2017). Renal glucose metabolism in normal physiological conditions and in diabetes. *Diabetes Res Clin Pract* 133, 1-9.

Alzeer, S., and Ellis, E.M. (2014). Metabolism of gamma hydroxybutyrate in human hepatoma HepG2 cells by the aldo-keto reductase AKR1A1. *Biochem Pharmacol* 92, 499-505.

Amara, F., Hafez, S., Orabi, A., El Etriby, A., Abdel Rahim, A.A., Zakaria, E., Koura, F., Talaat, F.M., Gawish, H., Attia, I., *et al.* (2019). Review of Diabetic Polyneuropathy: Pathogenesis, Diagnosis and Management According to the Consensus of Egyptian Experts. *Curr Diabetes Rev* 15, 340-345.

Asano, S., Himeno, T., Hayami, T., Motegi, M., Inoue, R., Nakai-Shimoda, H., Miura-Yura, E., Morishita, Y., Kondo, M., Tsunekawa, S., *et al.* (2019). Ranirestat Improved Nerve Conduction Velocities, Sensory Perception, and Intraepidermal Nerve Fiber Density in Rats with Overt Diabetic Polyneuropathy. *J Diabetes Res* 2019, 2756020.

Atkinson, M.A., Eisenbarth, G.S., and Michels, A.W. (2014). Type 1 diabetes. *Lancet* 383, 69-82.

Balendiran, G.K. (2009). Fibrates in the Chemical Action of Daunorubicin. *Curr Cancer Drug Tar* 9, 366-369.

Barthel, A., and Schmolli, D. (2003). Novel concepts in insulin regulation of hepatic gluconeogenesis. *Am J Physiol Endocrinol Metab* 285, E685-692.

Bellamy, L., Casas, J.P., Hingorani, A.D., and Williams, D. (2009). Type 2 diabetes mellitus after gestational diabetes: a systematic review and meta-analysis. *Lancet* 373, 1773-1779.

Benoy, M.P., and Elliott, K.A.C. (1937). The metabolism of lactic and pyruvic acids in normal and tumour tissues V. Synthesis of carbohydrate. *Biochem J* 31, 1268-1275.

## Reference

---

- Bergman, H., and Drury, D.R. (1938). The relationship of kidney function to the glucose utilization of the extra abdominal tissues. *Am J Physiol* 124, 279-284.
- Beyer-Mears, A., Murray, F.T., Del Val, M., Cruz, E., and Sciadini, M. (1988). Reversal of proteinuria by sorbinil, an aldose reductase inhibitor in spontaneously diabetic (BB) rats. *Pharmacology* 36, 112-120.
- Bjorkman, O., Felig, P., and Wahren, J. (1979). Gluconeogenesis by the Human-Kidney - Unique Stimulatory Effect of Fructose. *Clin Res* 27, A409-A409.
- Bohren, K.M., Bullock, B., Wermuth, B., and Gabbay, K.H. (1989). The aldo-keto reductase superfamily. cDNAs and deduced amino acid sequences of human aldehyde and aldose reductases. *J Biol Chem* 264, 9547-9551.
- Borg, R., Kuenen, J.C., Carstensen, B., Zheng, H., Nathan, D.M., Heine, R.J., Nerup, J., Borch-Johnsen, K., Witte, D.R., and Grp, A.S. (2011). HbA(1c) and mean blood glucose show stronger associations with cardiovascular disease risk factors than do postprandial glycaemia or glucose variability in persons with diabetes: the A1C-Derived Average Glucose (ADAG) study. *Diabetologia* 54, 69-72.
- Bredt, D.S., and Snyder, S.H. (1990). Isolation of nitric oxide synthetase, a calmodulin-requiring enzyme. *Proc Natl Acad Sci U S A* 87, 682-685.
- Bril, V., Hirose, T., Tomioka, S., Buchanan, R., and Grp, R.S. (2009). Ranirestat for the Management of Diabetic Sensorimotor Polyneuropathy. *Diabetes Care* 32, 1256-1260.
- Brownlee, M. (2001). Biochemistry and molecular cell biology of diabetic complications. *Nature* 414, 813-820.
- Buckingham, B., Wilson, D.M., Lecher, T., Hanas, R., Kaiserman, K., and Cameron, F. (2008). Duration of Nocturnal Hypoglycemia Before Seizures. *Diabetes Care* 31, 2110-2112.
- Chandramouli, V., Ekberg, K., Schumann, W.C., Kalhan, S.C., Wahren, J., and Landau, B.R. (1997). Quantifying gluconeogenesis during fasting. *Am J Physiol* 273, E1209-1215.
- Chen, Y.Q., Su, M., Walia, R.R., Hao, Q., Covington, J.W., and Vaughan, D.E. (1998). Sp1 sites mediate activation of the plasminogen activator inhibitor-1 promoter by glucose in vascular smooth muscle cells. *J Biol Chem* 273, 8225-8231.
- Cho, N.H., Shaw, J.E., Karuranga, S., Huang, Y., da Rocha Fernandes, J.D., Ohlrogge, A.W., and Malanda, B. (2018). IDF Diabetes Atlas: Global estimates of diabetes prevalence for 2017 and projections for 2045. *Diabetes Res Clin Pract* 138, 271-281.
- Chung, S.S.M., Ho, E.C.M., Lam, K.S.L., and Chung, S.K. (2003). Contribution of polyol pathway to diabetes-induced oxidative stress. *J Am Soc Nephrol* 14, S233-S236.

## Reference

---

Cogan, D.G., Kinoshita, J.H., Kador, P.F., Robison, G., Datilis, M.B., Cobo, L.M., and Kupfer, C. (1984). NIH conference. Aldose reductase and complications of diabetes. *Ann Intern Med* 101, 82-91.

Conjard, A., Martin, M., Guitton, J., Baverel, G., and Ferrier, B. (2001). Gluconeogenesis from glutamine and lactate in the isolated human renal proximal tubule: longitudinal heterogeneity and lack of response to adrenaline. *Biochem J* 360, 371-377.

Cornblath, M., and Ichord, R. (2000). Hypoglycemia in the neonate. *Semin Perinatol* 24, 136-149.

Craven, P.A., Studer, R.K., and DeRubertis, F.R. (1994). Impaired nitric oxide-dependent cyclic guanosine monophosphate generation in glomeruli from diabetic rats. Evidence for protein kinase C-mediated suppression of the cholinergic response. *J Clin Invest* 93, 311-320.

Cryer, P.E. (2007). Hypoglycemia, functional brain failure, and brain death. *J Clin Invest* 117, 868-870.

Cryer, P.E., Axelrod, L., Grossman, A.B., Heller, S.R., Montori, V.M., Seaquist, E.R., Service, F.J., and Endocrine, S. (2009). Evaluation and management of adult hypoglycemic disorders: an Endocrine Society Clinical Practice Guideline. *J Clin Endocrinol Metab* 94, 709-728.

Cukierman-Yaffe, T., Bosch, J., Jung, H., Punthakee, Z., and Gerstein, H.C. (2019). Hypoglycemia and Incident Cognitive Dysfunction: A Post Hoc Analysis From the ORIGIN Trial. *Diabetes Care* 42, 142-147.

Cunnane, S., Nugent, S., Roy, M., Courchesne-Loyer, A., Croteau, E., Tremblay, S., Castellano, A., Pifferi, F., Bocti, C., Paquet, N., *et al.* (2011). Brain fuel metabolism, aging, and Alzheimer's disease. *Nutrition* 27, 3-20.

Decker, J.H., Dochterman, L.W., Niquette, A.L., and Brej, M. (2012). Association of renal tubular hyaline droplets with lymphoma in CD-1 mice. *Toxicol Pathol* 40, 651-655.

Diabetes, C., Complications Trial Research, G., Nathan, D.M., Genuth, S., Lachin, J., Cleary, P., Crofford, O., Davis, M., Rand, L., and Siebert, C. (1993). The effect of intensive treatment of diabetes on the development and progression of long-term complications in insulin-dependent diabetes mellitus. *N Engl J Med* 329, 977-986.

Diniz, Y.S., Fernandes, A.A., Campos, K.E., Mani, F., Ribas, B.O., and Novelli, E.L. (2004). Toxicity of hypercaloric diet and monosodium glutamate: oxidative stress and metabolic shifting in hepatic tissue. *Food Chem Toxicol* 42, 313-319.

DiStefano, J.K., and Davis, B. (2019). Diagnostic and Prognostic Potential of AKR1B10 in Human Hepatocellular Carcinoma. *Cancers (Basel)* 11.

## Reference

---

- Dixit, S.G., Rani, P., Anand, A., Khatri, K., Chauhan, R., and Bharihoke, V. (2014). To study the effect of monosodium glutamate on histomorphometry of cortex of kidney in adult albino rats. *Ren Fail* 36, 266-270.
- Drummond, I.A., and Davidson, A.J. (2010). Zebrafish Kidney Development. *Method Cell Biol* 100, 233-260.
- Drury, D.R., Wick, A.N., and Mackay, E.M. (1950). Formation of Glucose by the Kidney. *Am J Physiol* 163, 655-661.
- Dryer, S.E. (2015). Glutamate receptors in the kidney. *Nephrol Dial Transplant* 30, 1630-1638.
- Du, J., Li, X.H., and Li, Y.J. (2016). Glutamate in peripheral organs: Biology and pharmacology. *Eur J Pharmacol* 784, 42-48.
- Duckworth, W., Abaira, C., Moritz, T., Reda, D., Emanuele, N., Reaven, P.D., Zieve, F.J., Marks, J., Davis, S.N., Hayward, R., *et al.* (2009). Glucose control and vascular complications in veterans with type 2 diabetes. *N Engl J Med* 360, 129-139.
- Dunlop, M. (2000). Aldose reductase and the role of the polyol pathway in diabetic nephropathy. *Kidney International* 58, S3-S12.
- El-Kabbani, O., Green, N.C., Lin, G., Carson, M., Narayana, S.V., Moore, K.M., Flynn, T.G., and DeLucas, L.J. (1994). Structures of human and porcine aldehyde reductase: an enzyme implicated in diabetic complications. *Acta Crystallogr D Biol Crystallogr* 50, 859-868.
- El-Kabbani, O., and Podjarny, A. (2007). Selectivity determinants of the aldose and aldehyde reductase inhibitor-binding sites. *Cellular and Molecular Life Sciences* 64, 1970-1978.
- Fagerberg, L., Hallstrom, B.M., Oksvold, P., Kampf, C., Djureinovic, D., Odeberg, J., Habuka, M., Tahmasebpour, S., Danielsson, A., Edlund, K., *et al.* (2014). Analysis of the Human Tissue-specific Expression by Genome-wide Integration of Transcriptomics and Antibody-based Proteomics. *Mol Cell Proteomics* 13, 397-406.
- Favetta, L.A., St John, E.J., King, W.A., and Betts, D.H. (2007). High levels of p66shc and intracellular ROS in permanently arrested early embryos. *Free Radic Biol Med* 42, 1201-1210.
- Feelisch, M. (1993). Biotransformation to nitric oxide of organic nitrates in comparison to other nitrovasodilators. *Eur Heart J* 14 Suppl I, 123-132.
- Fernando, V., Zheng, X., Walia, Y., Sharma, V., Letson, J., and Furuta, S. (2019). S-Nitrosylation: An Emerging Paradigm of Redox Signaling. *Antioxidants (Basel)* 8.

## Reference

---

Finfer, S., Liu, B., Chittock, D.R., Norton, R., Myburgh, J.A., McArthur, C., Mitchell, I., Foster, D., Dhingra, V., Henderson, W.R., *et al.* (2012). Hypoglycemia and risk of death in critically ill patients. *N Engl J Med* 367, 1108-1118.

Flannery, C.A., Choe, G.H., Cooke, K.M., Fleming, A.G., Radford, C.C., Kodaman, P.H., Jurczak, M.J., Kibbey, R.G., and Taylor, H.S. (2018). Insulin Regulates Glycogen Synthesis in Human Endometrial Glands Through Increased GYS2. *J Clin Endocr Metab* 103, 2843-2850.

Flynn, T.G., Green, N.C., Bhatia, M.B., and el-Kabbani, O. (1995). Structure and mechanism of aldehyde reductase. *Adv Exp Med Biol* 372, 193-201.

Forbes, J.M., and Cooper, M.E. (2013). Mechanisms of diabetic complications. *Physiol Rev* 93, 137-188.

Forman, H.J., Maiorino, M., and Ursini, F. (2010). Signaling functions of reactive oxygen species. *Biochemistry* 49, 835-842.

Fukumoto, S., Yamauchi, N., Moriguchi, H., Hippo, Y., Watanabe, A., Shibahara, J., Taniguchi, H., Ishikawa, S., Ito, H., Yamamoto, S., *et al.* (2005). Overexpression of the aldo-keto reductase family protein AKR1B10 is highly correlated with smokers' non-small cell lung carcinomas. *Clin Cancer Res* 11, 1776-1785.

Gabbay, K.H., Bohren, K.M., Morello, R., Bertin, T., Liu, J., and Vogel, P. (2010). Ascorbate synthesis pathway: dual role of ascorbate in bone homeostasis. *J Biol Chem* 285, 19510-19520.

Gerich, J.E. (1993). Control of glycaemia. *Baillieres Clin Endocrinol Metab* 7, 551-586.

Gerich, J.E., Meyer, C., Woerle, H.J., and Stumvoll, M. (2001). Renal gluconeogenesis - Its importance in human glucose homeostasis. *Diabetes Care* 24, 382-391.

Giardino, I., Edelstein, D., and Brownlee, M. (1994). Nonenzymatic glycosylation in vitro and in bovine endothelial cells alters basic fibroblast growth factor activity. A model for intracellular glycosylation in diabetes. *J Clin Invest* 94, 110-117.

Gu, L., Liang, X., Wang, L., Yan, Y., Ni, Z., Dai, H., Gao, J., Mou, S., Wang, Q., Chen, X., *et al.* (2012). Functional metabotropic glutamate receptors 1 and 5 are expressed in murine podocytes. *Kidney Int* 81, 458-468.

Hamada, Y., Araki, N., Horiuchi, S., and Hotta, N. (1996). Role of polyol pathway in nonenzymatic glycation. *Nephrol Dial Transpl* 11, 95-98.

Handy, D.E., and Loscalzo, J. (2012). Redox regulation of mitochondrial function. *Antioxid Redox Signal* 16, 1323-1367.

Hattersley, A., Bruining, J., Shield, J., Njolstad, P., and Donaghue, K.C. (2009). The diagnosis and management of monogenic diabetes in children and adolescents. *Pediatr Diabetes* 10 Suppl 12, 33-42.

## Reference

---

- He, J., Gao, H.X., Yang, N., Zhu, X.D., Sun, R.B., Xie, Y., Zeng, C.H., Zhang, J.W., Wang, J.K., Ding, F., *et al.* (2019). The aldose reductase inhibitor epalrestat exerts nephritic protection on diabetic nephropathy in db/db mice through metabolic modulation. *Acta Pharmacol Sin* **40**, 86-97.
- Heckler, K., and Kroll, J. (2017). Zebrafish as a Model for the Study of Microvascular Complications of Diabetes and Their Mechanisms. *Int J Mol Sci* **18**.
- Hempel, A., Maasch, C., Heintze, U., Lindschau, C., Dietz, R., Luft, F.C., and Haller, H. (1997). High glucose concentrations increase endothelial cell permeability via activation of protein kinase C alpha. *Circ Res* **81**, 363-371.
- Heringlake, S., Hofdmann, M., Fiebeler, A., Manns, M.P., Schmiegel, W., and Tannapfel, A. (2010). Identification and expression analysis of the aldo-ketoreductase1-B10 gene in primary malignant liver tumours. *J Hepatol* **52**, 220-227.
- Hers, H.G. (1956). [The mechanism of the transformation of glucose in fructose in the seminal vesicles]. *Biochim Biophys Acta* **22**, 202-203.
- Hess, D.T., Matsumoto, A., Kim, S.O., Marshall, H.E., and Stamler, J.S. (2005). Protein S-nitrosylation: purview and parameters. *Nat Rev Mol Cell Biol* **6**, 150-166.
- Hess, D.T., Patterson, S.I., Smith, D.S., and Skene, J.H.P. (1993). Neuronal Growth Cone Collapse and Inhibition of Protein Fatty Acylation by Nitric-Oxide. *Nature* **366**, 562-565.
- Hess, D.T., and Stamler, J.S. (2012). Regulation by S-nitrosylation of protein post-translational modification. *J Biol Chem* **287**, 4411-4418.
- Howarth, C., Gleeson, P., and Attwell, D. (2012). Updated energy budgets for neural computation in the neocortex and cerebellum. *J Cereb Blood Flow Metab* **32**, 1222-1232.
- Huang, L., He, R.Z., Luo, W.H., Zhu, Y.S., Li, J., Tan, T., Zhang, X., Hu, Z., and Luo, D.X. (2016). Aldo-Keto Reductase Family 1 Member B10 Inhibitors: Potential Drugs for Cancer Treatment. *Recent Pat Anti-Canc* **11**, 184-196.
- Hyndman, D., Bauman, D.R., Heredia, V.V., and Penning, T.M. (2003). The aldo-keto reductase superfamily homepage. *Chem Biol Interact* **143-144**, 621-631.
- Jaubert, A.M., Penot, G., Niang, F., Durant, S., and Forest, C. (2012). Rapid nitration of adipocyte phosphoenolpyruvate carboxykinase by leptin reduces glyceroneogenesis and induces fatty acid release. *Plos One* **7**, e40650.
- Jiang, G., and Zhang, B.B. (2003). Glucagon and regulation of glucose metabolism. *Am J Physiol Endocrinol Metab* **284**, E671-678.
- Jiang, H., Shen, Y.M., Quinn, A.M., and Penning, T.M. (2005). Competing roles of cytochrome P450 1A1/1B1 and aldo-keto reductase 1A1 in the metabolic activation of

## Reference

---

(+/-)-7,8-dihydroxy-7,8-dihydro-benzo[a]pyrene in human bronchoalveolar cell extracts. *Chem Res Toxicol* 18, 365-374.

Jiang, H., Vudathala, D.K., Blair, I.A., and Penning, T.M. (2006). Competing roles of aldo-keto reductase 1A1 and cytochrome P4501B1 in benzo[a]pyrene-7,8-diol activation in human bronchoalveolar H358 cells: role of AKRs in P4501B1 induction. *Chem Res Toxicol* 19, 68-78.

K. Sing, A.P. (2005). Alteration in some antioxidant enzymes in cardiac tissue upon monosodium glutamate administration to adult male mice. *Indian J Clin Biochem* 20, 43-46.

Kato, N., Yashima, S., Suzuki, T., Nakayama, Y., and Jomori, T. (2003). Long-term treatment with fidarestat suppresses the development of diabetic retinopathy in STZ-induced diabetic rats. *J Diabetes Complications* 17, 374-379.

Katsarou, A., Gudbjornsdottir, S., Rawshani, A., Dabelea, D., Bonifacio, E., Anderson, B.J., Jacobsen, L.M., Schatz, D.A., and Lernmark, A. (2017). Type 1 diabetes mellitus. *Nat Rev Dis Primers* 3, 17016.

Kinoshita, J.H., and Nishimura, C. (1988). The Involvement of Aldose Reductase in Diabetic Complications. *Diabetes Metab Rev* 4, 323-337.

Kittah, N.E., and Vella, A. (2017). MANAGEMENT OF ENDOCRINE DISEASE: Pathogenesis and management of hypoglycemia. *Eur J Endocrinol* 177, R37-R47.

Kornberg, M.D., Sen, N., Hara, M.R., Juluri, K.R., Nguyen, J.V.K., Snowman, A.M., Law, L., Hester, L.D., and Snyder, S.H. (2010). GAPDH mediates nitrosylation of nuclear proteins. *Nat Cell Biol* 12, 1094-U1089.

Kurahashi, T., Kwon, M., Homma, T., Saito, Y., Lee, J., Takahashi, M., Yamada, K.I., Miyata, S., and Fujii, J. (2014). Reductive detoxification of acrolein as a potential role for aldehyde reductase (AKR1A) in mammals. *Biochem Bioph Res Co* 452, 136-141.

Lai, C.W., Chen, H.L., Tu, M.Y., Lin, W.Y., Rohrig, T., Yang, S.H., Lan, Y.W., Chong, K.Y., and Chen, C.M. (2017). A novel osteoporosis model with ascorbic acid deficiency in Akr1A1 gene knockout mice. *Oncotarget* 8, 7357-7369.

Li, D., Zhang, Q., Zhou, L., and Liu, R. (2013). [Effect of AKR1A1 knock-down on H<sub>2</sub>O<sub>2</sub> and 4-hydroxynonenal-induced cytotoxicity in human 1321N1 astrocytoma cells]. *Xi Bao Yu Fen Zi Mian Yi Xue Za Zhi* 29, 273-276.

Li, F., Sonveaux, P., Rabbani, Z.N., Liu, S.L., Yan, B., Huang, Q., Vujaskovic, Z., Dewhirst, M.W., and Li, C.Y. (2007). Regulation of HIF-1 alpha stability through S-nitrosylation. *Mol Cell* 26, 63-74.

Li, Q., Hwang, Y.Y.C., Ananthakrishnan, R., Oates, P.J., Guberski, D., and Ramasamy, R. (2008). Polyol pathway and modulation of ischemia-reperfusion injury in Type 2 diabetic BBZ rat hearts. *Cardiovasc Diabetol* 7.

## Reference

---

- Li, Q.R., Wang, Z., Zhou, W., Fan, S.R., Ma, R., Xue, L., Yang, L., Li, Y.S., Tan, H.L., Shao, Q.H., *et al.* (2016). Epalrestat protects against diabetic peripheral neuropathy by alleviating oxidative stress and inhibiting polyol pathway. *Neural Regen Res* 11, 345-351.
- Lin, Q.Y., Song, B., Huang, H., and Li, T.H. (2010). Optimization of selected cultivation parameters for *Cordyceps guangdongensis*. *Lett Appl Microbiol* 51, 219-225.
- Little, S.A., Speight, J., Leelarathna, L., Walkinshaw, E., Tan, H.K., Bowes, A., Lubina-Solomon, A., Chadwick, T.J., Stocken, D.D., Brennand, C., *et al.* (2018). Sustained Reduction in Severe Hypoglycemia in Adults With Type 1 Diabetes Complicated by Impaired Awareness of Hypoglycemia: Two-Year Follow-up in the HypoCOMPASS Randomized Clinical Trial. *Diabetes Care* 41, 1600-1607.
- Liu, Z.W., Yan, R.L., Al-Salman, A., Shen, Y., Bu, Y.W., Ma, J., Luo, D.X., Huang, C.F., Jiang, Y.Y., Wilber, A., *et al.* (2012). Epidermal growth factor induces tumour marker AKR1B10 expression through activator protein-1 signalling in hepatocellular carcinoma cells. *Biochem J* 442, 273-282.
- Lodd, E., Wiggerhauser, L.M., Morgenstern, J., Fleming, T.H., Poschet, G., Buttner, M., Tabler, C.T., Wohlfart, D.P., Nawroth, P.P., and Kroll, J. (2019). The combination of loss of glyoxalase1 and obesity results in hyperglycemia. *JCI Insight* 4.
- Lorenzi, M. (2007). The Polyol Pathway as a Mechanism for Diabetic Retinopathy: Attractive, Elusive, and Resilient. *Exp Diabetes Res*.
- Lou, M.F., Xu, G.T., Zigler, S., and York, B. (1996). Inhibition of naphthalene cataract in rats by aldose reductase inhibitors. *Curr Eye Res* 15, 423-432.
- Ma, J., Luo, D.X., Huang, C.F., Shen, Y., Bu, Y.W., Markwell, S., Gao, J., Liu, J.H., Zu, X.Y., Cao, Z., *et al.* (2012). AKR1B10 overexpression in breast cancer: Association with tumor size, lymph node metastasis and patient survival and its potential as a novel serum marker. *Int J Cancer* 131, E862-E871.
- MacLeod, A.K., Kelly, V.P., Higgins, L.G., Kelleher, M.O., Price, S.A., Bigley, A.L., Betton, G.R., and Hayes, J.D. (2010). Expression and localization of rat aldo-keto reductases and induction of the 1B13 and 1D2 isoforms by phenolic antioxidants. *Drug Metab Dispos* 38, 341-346.
- Markus, H.B., Raducha, M., and Harris, H. (1983). Tissue distribution of mammalian aldose reductase and related enzymes. *Biochem Med* 29, 31-45.
- Mergenthaler, P., Lindauer, U., Dienel, G.A., and Meisel, A. (2013). Sugar for the brain: the role of glucose in physiological and pathological brain function. *Trends Neurosci* 36, 587-597.
- Murillo-Carretero, M., Torroglosa, A., Castro, C., Villalobo, A., and Estrada, C. (2009). S-Nitrosylation of the epidermal growth factor receptor: A regulatory mechanism of receptor tyrosine kinase activity. *Free Radical Bio Med* 46, 471-479.



## Reference

---

- Nakamura, T., and Lipton, S.A. (2013). Emerging role of protein-protein transnitrosylation in cell signaling pathways. *Antioxid Redox Signal* 18, 239-249.
- Niang, F., Benelli, C., Ribiere, C., Collinet, M., Mehebik-Mojaat, N., Penot, G., Forest, C., and Jaubert, A.M. (2011). Leptin induces nitric oxide-mediated inhibition of lipolysis and glyceroneogenesis in rat white adipose tissue. *J Nutr* 141, 4-9.
- Oates, P.J. (2008). Aldose reductase, still a compelling target for diabetic neuropathy. *Current Drug Targets* 9, 14-36.
- Obrosova, I.G., Chung, S.S.M., and Kador, P.F. (2010). Diabetic cataracts: mechanisms and management. *Diabetes-Metab Res* 26, 172-180.
- Olsen, A.S., Sarras, M.P., and Intine, R.V. (2010). Limb regeneration is impaired in an adult zebrafish model of diabetes mellitus. *Wound Repair Regen* 18, 532-542.
- Pagliara, A.S., and Goodman, A.D. (1970). Relation of renal cortical gluconeogenesis, glutamate content, and production of ammonia. *J Clin Invest* 49, 1967-1974.
- Palackal, N.T., Lee, S.H., Harvey, R.G., Blair, I.A., and Penning, T.M. (2002). Activation of polycyclic aromatic hydrocarbon trans-dihydrodiol proximate carcinogens by human aldo-keto reductase (AKR1C) enzymes and their functional overexpression in human lung carcinoma (A549) cells. *J Biol Chem* 277, 24799-24808.
- Paul, S., Ali, A., and Katare, R. (2020). Molecular complexities underlying the vascular complications of diabetes mellitus - A comprehensive review. *J Diabetes Complications* 34, 107613.
- Penning, T.M. (2015). The aldo-keto reductases (AKRs): Overview. *Chem Biol Interact* 234, 236-246.
- Penning, T.M., Burczynski, M.E., Jez, J.M., Hung, C.F., Lin, H.K., Ma, H., Moore, M., Palackal, N., and Ratnam, K. (2000). Human 3 $\alpha$ -hydroxysteroid dehydrogenase isoforms (AKR1C1-AKR1C4) of the aldo-keto reductase superfamily: functional plasticity and tissue distribution reveals roles in the inactivation and formation of male and female sex hormones. *Biochem J* 351, 67-77.
- Petersen, M.C., Vatner, D.F., and Shulman, G.I. (2017). Regulation of hepatic glucose metabolism in health and disease. *Nature Reviews Endocrinology* 13, 572-587.
- Petersmann, A., Muller-Wieland, D., Muller, U.A., Landgraf, R., Nauck, M., Freckmann, G., Heinemann, L., and Schleicher, E. (2019). Definition, Classification and Diagnosis of Diabetes Mellitus. *Exp Clin Endocrinol Diabetes* 127, S1-S7.
- Pina, A.F., Borges, D.O., Meneses, M.J., Branco, P., Birne, R., Vilasi, A., and Macedo, M.P. (2020). Insulin: Trigger and Target of Renal Functions. *Front Cell Dev Biol* 8, 519.

## Reference

---

- Puliti, A., Rossi, P.I., Caridi, G., Corbelli, A., Ikehata, M., Armelloni, S., Li, M., Zennaro, C., Conti, V., Vaccari, C.M., *et al.* (2011). Albuminuria and glomerular damage in mice lacking the metabotropic glutamate receptor 1. *Am J Pathol* **178**, 1257-1269.
- Quinn, P.G., and Yeagley, D. (2005). Insulin regulation of PEPCK gene expression: a model for rapid and reversible modulation. *Curr Drug Targets Immune Endocr Metabol Disord* **5**, 423-437.
- Raj, D.S., Welbourne, T., Dominic, E.A., Waters, D., Wolfe, R., and Ferrando, A. (2005). Glutamine kinetics and protein turnover in end-stage renal disease. *Am J Physiol Endocrinol Metab* **288**, E37-46.
- Ramasamy, R., and Goldberg, I.J. (2010). Aldose Reductase and Cardiovascular Diseases, Creating Human-Like Diabetic Complications in an Experimental Model. *Circulation Research* **106**, 1449-1458.
- Rittner, H.L., Hafner, V., Klimiuk, P.A., Szweda, L.I., Goronzy, J.J., and Weyand, C.M. (1999). Aldose reductase functions as a detoxification system for lipid peroxidation products in vasculitis. *J Clin Invest* **103**, 1007-1013.
- Rizzo, M.A., and Piston, D.W. (2003). Regulation of beta cell glucokinase by S-nitrosylation and association with nitric oxide synthase. *J Cell Biol* **161**, 243-248.
- Roglic, G., and World Health Organization (2016). Global report on diabetes (Geneva, Switzerland: World Health Organization).
- Rothman, D.L., Magnusson, I., Katz, L.D., Shulman, R.G., and Shulman, G.I. (1991). Quantitation of hepatic glycogenolysis and gluconeogenesis in fasting humans with <sup>13</sup>C NMR. *Science* **254**, 573-576.
- Ruderman, N.B. (1975). Muscle amino acid metabolism and gluconeogenesis. *Annu Rev Med* **26**, 245-258.
- Rui, L. (2014). Energy metabolism in the liver. *Compr Physiol* **4**, 177-197.
- Saremi, A., Bahn, G.D., Reaven, P.D., and Vadt (2016). A Link Between Hypoglycemia and Progression of Atherosclerosis in the Veterans Affairs Diabetes Trial (VADT). *Diabetes Care* **39**, 448-454.
- Sato, S., Kitamura, H., Ghazizadeh, M., Adachi, A., Sasaki, Y., Ishizaki, M., Inoue, K., Wakamatsu, K., and Sugisaki, Y. (2005). Occurrence of hyaline droplets in renal biopsy specimens: an ultrastructural study. *Med Mol Morphol* **38**, 63-71.
- Schade, S.Z., Early, S.L., Williams, T.R., Kezdy, F.J., Heinrikson, R.L., Grimshaw, C.E., and Doughty, C.C. (1990). Sequence analysis of bovine lens aldose reductase. *J Biol Chem* **265**, 3628-3635.
- Schmohl, F., Peters, V., Schmitt, C.P., Poschet, G., Buttner, M., Li, X., Weigand, T., Poth, T., Volk, N., Morgenstern, J., *et al.* (2019). CNDP1 knockout in zebrafish alters the

## Reference

---

amino acid metabolism, restrains weight gain, but does not protect from diabetic complications. *Cell Mol Life Sci* 76, 4551-4568.

Schumacher, D., Morgenstern, J., Oguchi, Y., Volk, N., Kopf, S., Groener, J.B., Nawroth, P.P., Fleming, T., and Freichel, M. (2018). Compensatory mechanisms for methylglyoxal detoxification in experimental & clinical diabetes. *Mol Metab* 18, 143-152.

Scotcher, D., Jones, C., Posada, M., Rostami-Hodjegan, A., and Galetin, A. (2016). Key to Opening Kidney for In Vitro-In Vivo Extrapolation Entrance in Health and Disease: Part I: In Vitro Systems and Physiological Data. *Aaps J* 18, 1067-1081.

Sharma, A., Prasongwattana, V., Cha'on, U., Selmi, C., Hipkayo, W., Boonnate, P., Pethlert, S., Titipungul, T., Intarawichian, P., Warasawapati, S., *et al.* (2013). Monosodium Glutamate (MSG) Consumption Is Associated with Urolithiasis and Urinary Tract Obstruction in Rats. *Plos One* 8.

Sobngwi, E., Mauvais-Jarvis, F., Vexiau, P., Mbanya, J.C., and Gautier, J.F. (2002). Diabetes in Africans. Part 2: Ketosis-prone atypical diabetes mellitus. *Diabetes Metab* 28, 5-12.

Srivastava, S., Chandra, A., Bhatnagar, A., Srivastava, S.K., and Ansari, N.H. (1995). Lipid peroxidation product, 4-hydroxynonenal and its conjugate with GSH are excellent substrates of bovine lens aldose reductase. *Biochem Biophys Res Commun* 217, 741-746.

Srivastava, S.K., Petrash, J.M., Sadana, I.J., Ansari, N.H., and Partridge, C.A. (1982). Susceptibility of Aldehyde and Aldose Reductases of Human-Tissues to Aldose Reductase Inhibitors. *Curr Eye Res* 2, 407-410.

Srivastava, S.K., Ramana, K.V., and Bhatnagar, A. (2005). Role of aldose reductase and oxidative damage in diabetes and the consequent potential for therapeutic options. *Endocrine Reviews* 26, 380-392.

Stomberski, C.T., Anand, P., Venetos, N.M., Hausladen, A., Zhou, H.L., Premont, R.T., and Stamler, J.S. (2019). AKR1A1 is a novel mammalian S-nitroso-glutathione reductase. *J Biol Chem* 294, 18285-18293.

Stomnaroska-Damcevski, O., Petkovska, E., Jancevska, S., and Danilovski, D. (2015). Neonatal Hypoglycemia: A Continuing Debate in Definition and Management. *Pril (Makedon Akad Nauk Umet Odd Med Nauki)* 36, 91-97.

Stumvoll, M., Meyer, C., Kreider, M., Perriello, G., and Gerich, J. (1998). Effects of glucagon on renal and hepatic glutamine gluconeogenesis in normal postabsorptive humans. *Metabolism* 47, 1227-1232.

Stumvoll, M., Perriello, G., Meyer, C., and Gerich, J. (1999). Role of glutamine in human carbohydrate metabolism in kidney and other tissues. *Kidney Int* 55, 778-792.

## Reference

---

Suzen, S., and Buyukbingol, E. (2003). Recent studies of aldose reductase enzyme inhibition for diabetic complications. *Curr Med Chem* 10, 1329-1352.

Szwergold, B.S., Kappler, F., and Brown, T.R. (1990). Identification of Fructose 3-Phosphate in the Lens of Diabetic Rats. *Science* 247, 451-454.

Takahashi, M., Fujii, J., Teshima, T., Suzuki, K., Shiba, T., and Taniguchi, N. (1993). Identity of a major 3-deoxyglucosone-reducing enzyme with aldehyde reductase in rat liver established by amino acid sequencing and cDNA expression. *Gene* 127, 249-253.

Takahashi, M., Miyata, S., Fujii, J., Inai, Y., Ueyama, S., Araki, M., Soga, T., Fujinawa, R., Nishitani, C., Ariki, S., *et al.* (2012). In vivo role of aldehyde reductase. *Biochim Biophys Acta* 1820, 1787-1796.

Tesfaye, N., and Seaquist, E.R. (2010). Neuroendocrine responses to hypoglycemia. *Ann N Y Acad Sci* 1212, 12-28.

Tilton, R.G., Chang, K., Pugliese, G., Eades, D.M., Province, M.A., Sherman, W.R., Kilo, C., and Williamson, J.R. (1989). Prevention of hemodynamic and vascular albumin filtration changes in diabetic rats by aldose reductase inhibitors. *Diabetes* 38, 1258-1270.

Toyoda, F., Tanaka, Y., Ota, A., Shimmura, M., Kinoshita, N., Takano, H., Matsumoto, T., Tsuji, J., and Kakehashi, A. (2014). Effect of Ranirestat, a New Aldose Reductase Inhibitor, on Diabetic Retinopathy in SDT Rats. *Journal of Diabetes Research*.

UKPDS (1998). Intensive blood-glucose control with sulphonylureas or insulin compared with conventional treatment and risk of complications in patients with type 2 diabetes (UKPDS 33). UK Prospective Diabetes Study (UKPDS) Group. *Lancet* 352, 837-853.

Vargas, E., Podder, V., and Carrillo Sepulveda, M.A. (2020). Physiology, Glucose Transporter Type 4 (GLUT4). In *StatPearls* (Treasure Island (FL)).

Vu, C.U., Siddiqui, J.A., Wadensweiler, P., Gayen, J.R., Avolio, E., Bandyopadhyay, G.K., Biswas, N., Chi, N.W., O'Connor, D.T., and Mahata, S.K. (2014). Nicotinic acetylcholine receptors in glucose homeostasis: the acute hyperglycemic and chronic insulin-sensitive effects of nicotine suggest dual opposing roles of the receptors in male mice. *Endocrinology* 155, 3793-3805.

Wang, Q., Wang, D., Shibata, S., Ji, T., Zhang, L., Zhang, R., Yang, H., Ma, L., and Jiao, J. (2019). Group I metabotropic glutamate receptor activation induces TRPC6-dependent calcium influx and RhoA activation in cultured human kidney podocytes. *Biochem Biophys Res Commun* 511, 374-380.

Wells, L., and Hart, G.W. (2003). O-GlcNAc turns twenty: functional implications for post-translational modification of nuclear and cytosolic proteins with a sugar. *FEBS Lett* 546, 154-158.

## Reference

---

- Wermuth, B., Omar, A., Forster, A., di Francesco, C., Wolf, M., von Wartburg, J.P., Bullock, B., and Gabbay, K.H. (1987). Primary structure of aldehyde reductase from human liver. *Prog Clin Biol Res* 232, 297-307.
- West, M.B., Hill, B.G., Xuan, Y.T., and Bhatnagar, A. (2006). Protein glutathiolation by nitric oxide: an intracellular mechanism regulating redox protein modification. *Faseb J* 20, 1715-+.
- Whitmer, R.A., Karter, A.J., Yaffe, K., Quesenberry, C.P., Jr., and Selby, J.V. (2009). Hypoglycemic episodes and risk of dementia in older patients with type 2 diabetes mellitus. *JAMA* 301, 1565-1572.
- Wiggenhauser, L.M., Qi, H., Stoll, S.J., Metzger, L., Bennewitz, K., Poschet, G., Krenning, G., Hillebrands, J.L., Hammes, H.P., and Kroll, J. (2020). Activation of retinal angiogenesis in hyperglycemic *pdx1* (-/-) zebrafish mutants. *Diabetes*.
- Wijermars, L.G.M., Schaapherder, A.F., George, T., Sinharoy, P., and Gross, E.R. (2018). Association of Impaired Reactive Aldehyde Metabolism with Delayed Graft Function in Human Kidney Transplantation. *Oxid Med Cell Longev* 2018, 3704129.
- Williams, B., Gallacher, B., Patel, H., and Orme, C. (1997). Glucose-induced protein kinase C activation regulates vascular permeability factor mRNA expression and peptide production by human vascular smooth muscle cells in vitro. *Diabetes* 46, 1497-1503.
- Wu, C., Khan, S.A., and Lange, A.J. (2005). Regulation of glycolysis-role of insulin. *Exp Gerontol* 40, 894-899.
- Xiao, J.H., Chen, D.X., Liu, J.W., Liu, Z.L., Wan, W.H., Fang, N., Xiao, Y., Qi, Y., and Liang, Z.Q. (2004). Optimization of submerged culture requirements for the production of mycelial growth and exopolysaccharide by *Cordyceps jiangxiensis* JXPJ 0109. *J Appl Microbiol* 96, 1105-1116.
- Yanai, H., Adachi, H., Katsuyama, H., Moriyama, S., Hamasaki, H., and Sako, A. (2015). Causative anti-diabetic drugs and the underlying clinical factors for hypoglycemia in patients with diabetes. *World J Diabetes* 6, 30-36.
- Ye, Q., Hyndman, D., Green, N.C., Li, L., Jia, Z., and Flynn, T.G. (2001). The crystal structure of an aldehyde reductase Y50F mutant-NADP complex and its implications for substrate binding. *Chem Biol Interact* 130-132, 651-658.
- Yip, J., Geng, X., Shen, J., and Ding, Y. (2016). Cerebral Gluconeogenesis and Diseases. *Front Pharmacol* 7, 521.
- Yu, Y., Fuscoe, J.C., Zhao, C., Guo, C., Jia, M., Qing, T., Bannon, D.I., Lancashire, L., Bao, W., Du, T., *et al.* (2014). A rat RNA-Seq transcriptomic BodyMap across 11 organs and 4 developmental stages. *Nat Commun* 5, 3230.

## Reference

---

Yue, F., Cheng, Y., Breschi, A., Vierstra, J., Wu, W.S., Ryba, T., Sandstrom, R., Ma, Z.H., Davis, C., Pope, B.D., *et al.* (2014). A comparative encyclopedia of DNA elements in the mouse genome. *Nature* 515, 355-+.

Zhang, C., Liu, C., Li, D., Yao, N., Yuan, X., Yu, A., Lu, C., and Ma, X. (2010). Intracellular redox imbalance and extracellular amino acid metabolic abnormality contribute to arsenic-induced developmental retardation in mouse preimplantation embryos. *J Cell Physiol* 222, 444-455.

Zhou, H.L., Zhang, R., Anand, P., Stomberski, C.T., Qian, Z., Hausladen, A., Wang, L., Rhee, E.P., Parikh, S.M., Karumanchi, S.A., *et al.* (2019). Metabolic reprogramming by the S-nitroso-CoA reductase system protects against kidney injury. *Nature* 565, 96-100.

Zinman, B., Marso, S.P., Christiansen, E., Calanna, S., Rasmussen, S., Buse, J.B., and Investigators, L.P.C.o.b.o.t.L.T. (2018). Hypoglycemia, Cardiovascular Outcomes, and Death: The LEADER Experience. *Diabetes Care* 41, 1783-1791.

## 7 CURRICULUM VITAE

### Personal Information

Name:	Xiaogang Li, male
Date of birth:	12.12.1987
Place of birth:	Daqing, Heilongjiang, China
Marital status:	Unmarried
Father:	Lin Li
Mother:	Guiru Sun

### Primary School Education

09.1994 – 16.1999	Dorbod Mongol Autonomous County No. 3 Primary school Daqing, Heilongjiang, China
09.1999 – 06.2002	Dorbod Mongol Autonomous County No. 2 Middle school Daqing, Heilongjiang, China
09.2002 – 06.2005	Dorbod Mongol Autonomous County No. 1 High school Daqing, Heilongjiang, China

### University Education

09.2006 – 07.2010	Bachelor of Engineering, School of Life Science, Heilongjiang University, Heilongjiang Province, China
09.2011 – 06.2014	Master of Science, Key Laboratory of cell engineering of Guizhou Province, Zunyi Medical College, Guizhou Province, China
12.2016 – Present	Medical Faculty Mannheim, Heidelberg University, Germany

## 8 ACKNOWLEDGEMENTS

I thank everyone who contributed to the successful accomplishment of this work.

At first, my special thanks go to Prof. Dr. Jens Kroll, who made it possible for me to carry out my Dr.sc.hum. thesis in his lab, for the patient guidance, encouragement and advice he has provided throughout all my research.

Then, I want to give my sincere thanks to the whole Kroll-Lab team, which has accompanied and assisted me in the past three years. Katrin Bennewitz, Dr. Elisabeth Lodd, Dr. Bowen Lou, Silas Soleymani, Dr. Felix Schmöhl, Utsho Ali-Hader, Mike Boger, Haozhe Qi (Ryan), David Wohlfart, and everyone else, who has brought the laboratory to life, thank you.

Last, I also thank Dr. Gernot Poschet, Elena Heidenreich, Dr. Carsten Sticht, Dr. Carolina De La Torre, Dr. Nadine Volk, Dr. Tanja Poth, Dr. Ingrid Hausser, Dr. Thomas Fleming, Dr. Jakob Morgenstern, Prof. Dr. Karen Bieback, Prof. Dr. Peter Paul Nawroth, Prof. Dr. Hans-Peter Hammes, Prof. Dr. Ilse Hofmann and the Live Cell Imaging Mannheim, for all the technical sustentation, excellent instruction and cooperation. Furthermore, I would like to thank all the support from the SFB1118, the GRK 1874 DIAMICOM and China Scholarship Council (CSC).